DEVELOPMENT OF SIMULATION-BASED THORACIC INJURY PROBABILITY FUNCTION FOR ELDERLY FEMALE OCCUPANTS IN SIDE IMPACT

Hisaki Sugaya, **Takayuki Kawabuchi**, **Yukou Takahashi**,

Honda R&D Co., Ltd. Innovative Research Excellence, Tochigi, Japan

Craig Markusic, **Skye Malcolm**,

Honda Development & Manufacturing of America, LLC., Ohio, United States

Amanda Agnew, **Yun-Seok Kang**, **John Bolte IV**

Injury Biomechanics Research Center (IBRC), The Ohio State University, Ohio, United States

Paper Number 23-0090

ABSTRACT

Despite the high morbidity of elderly female car occupants in near side crashes, not many studies have been performed to predict the probability of injury to this population. A methodology to compensate for limitations in the amount of available biomechanical data is essential to derive an injury probability function for elderly females in near-side crashes. This study aims to establish a methodology to develop an injury probability function (IPF) by means of computational impact simulations using a human body model (HBM) that also includes variability in the material properties of human ribs. Focus was given to the prediction of rib fractures because of their high frequency in these near-side crash scenarios.

Variation in the material properties of ribs from the 5th percentile elderly female population were applied to a HBM developed in a past study by applying eight different stress-strain curves. The variability in the prediction of rib fracture was accounted for using a probabilistic approach derived from the literature. This altered HBM was then scaled to the size and mass of subjects used in experimental studies. The predicted thoracic deflection was validated against both isolated lateral thoracic impacts and side impact sled tests which included a side-airbag and a pretensioning seatbelt. The probability of three or more rib fractures predicted by the probabilistic approach was used to validate the altered HBM against the previous PMHS experiments. Additional sled test simulations were conducted with reduced energy by decreasing the impact velocity and also by varying the use of the airbag. IPF predicting the probability of rib fractures was developed using the logistic regression and compared between the original dataset based on the PMHS sled tests and the modified dataset created by the additional simulations conducted at reduced severity.

Chest deflection from the experimental thoracic impactor tests fell within the predicted range from the HBM simulations. In addition, chest deflection from the majority of the PMHS sled experiments that were simulated fell within the predicted range by the HBM. The probability of 3+ rib fractures was 100% for both the simulations and the experiments against realistic lateral sled tests. The IPF developed from the modified dataset predicted a significantly lower probability of rib fracture than that from the original dataset.

This study qualitatively evaluated the idea of predicting injury probability for a specific population by representing the variability in the material properties of ribs to an HBM, specifically a near-side impact load case for 5th percentile elderly female occupants. The effect of the geometry, such as the shape of the rib cage and rib thickness, was not reproduced in this study. The method used to derive the IPFs could also be done for other load cases and populations.

INTRODUCTION

In the united states, approximately 2.28 million occupants were injured in car crashes in 2020 according to the accident analysis. [1] A previous study done by NHTSA analyzed the National Automotive Sampling System Crashworthiness Data System (NASS-CDS) and found that the percentage of drivers sustaining Maximum Abbreviated Injury Scale (AIS) 4+ injuries relative to the number of drivers involved in accidents is significantly higher for the elderly population of 65 years old and older than the age group between 25 and 44 years old, accounting for 1.85% and 0.76%, respectively. The percentage of the elderly population becomes even larger, specifically for left-side impacts without rollover, comprising the largest percentage of all crash modes [2]. This suggests that protection of elderly drivers involved in left-side impacts is crucial.

Further investigation of the side-impact elderly crash data from the previous study showed that elderly female occupants are more likely to suffer injuries than males, especially to the thoracic ribs. In near-side impacts, the probability of AIS 3+ injuries to the thorax and the ribs was significantly higher for females than for males within the elderly population.[3] This suggests that elderly female drivers in near-side impacts are a more susceptible group to thoracic injuries such as rib fractures than elderly male drivers. Therefore, this study focused on thoracic injuries sustained by elderly female occupants.

In a previous study focused on elderly female biomechanical response, whole single rib bending tests were performed, showing that the force at a fracture of female ribs was significantly lower than those of male ribs [4], which could point to the elderly female being more fragile than the elderly male. Due to the growing importance for the protection of elderly female occupants in near-side impacts, several studies have investigated this impact configuration. At the full-scale level, Wood et al. [5] developed a thoracic injury probability function (IPF) for elderly female in side impacts using a rigid wall and elderly post-mortem human surrogates (PMHS), with six female and two male subjects. Based on the thoracic IPF, a normalized half deflection (NHD) value of 0.23 was proposed for a 50% probability of AIS3+ thoracic injury. A more recent study by Shurtz et al. [6] and Bolte et al. [7] conducted side impact sled tests utilizing a mass productionbased restraint system with ten elderly female PMHS and a Delta-V of approximately 28 km/h. These sled tests produced NHDs from 0.05 – 0.13 and AIS 3+ thoracic injuries for eight of the ten subjects that reached AIS 3+. These studies reveal differences in the relationship between NHD and the occurrence of AIS3+ thoracic injury. One possible explanation for this is the influence of different boundary conditions. However, there has not been a study of applying the IPF using vehicle boundary conditions. Therefore, the objective of this study was to investigate a method to develop an IPF for thoracic injury to elderly female occupants given real-world vehicle boundary conditions.

In order to accurately predict injury probability in realistic crash scenarios, especially when focusing on specific crash conditions, a method that complements the limited number of PMHS experimental data is needed. Due to the small number of samples, it is difficult to predict individual variation solely based on experimental results. In this study, a methodology to complement the limitations by means of computer simulation was used. The body size of PMHS can be matched from subject data, however, material properties are not known for each rib from each individual subjects. In this study, these unknown material properties were modeled by including variation across a number of physical material property coupon tests. The purpose of this study was to investigate a method to improve the IPF for thoracic injury to elderly female occupants using crash simulation with a human body model that applied variations to the material properties of human rib cortical bone tissue, which comprises the major component of the stiffness of the thoracic cage.

METHOD

The methods used to improve the thoracic IPF for this crash scenario began by developing the HBM to include experimental cortical bone properties. Once the model was updated it was validated against both impactor and sled tests with real-world boundary conditions. Finally, the model was then used to create the new thoracic IPF.

Development of a Variability Human Body Model (vHBM)

The HBM used in this study was an inhouse HBM developed by Sugaya et al. [8] representing an elderly female with the size of 5th % American female (AF) using LS-DYNA R7.1.2. This study developed a variability human body model (vHBM) that reflects variability in the material property of rib cortical bone using MATERIAL TYPE 124 (*MAT_PLASTICITY_COMPRESSION_TENSION).[9] The variability of the material property was reproduced by giving variation to the modulus of elasticity, yield stress, and slope in the plastic region determined from rib bone material data of eight female ribs over 61 years old described by Katzenberger et al. [10] and

Kemper et al. [11]. The fracture probability of each of the "true" ribs, the first seven which attach to the sternum, was calculated using maximum strain values from the literature as shown in appendix A. As shown in Figure 1, the relationship between the fracture strain and the fracture probability (fracture probability equation) was developed using the survival method. Using the fracture probability equation, the probability of fracture to 3 or more ribs was calculated using the probabilistic analysis by Forman et al. [12] using a generalized form of a binomial probability model Pr(X) with equation (1).

$$\Pr(X) = \sum_{i=1}^{\binom{N}{X}} \left(\prod_{k \in C_i} p_j \right) \left(\prod_{k \in \bar{C}_i} (1 - p_k) \right) \qquad Equation\ (1)$$

where Pj is the fracture probability at the j th site (rib)
N is the number of potential fracture sites (number of ribs)
Ci is a vector containing the ith combination of X site indices
$\bar{C}\imath$ is a vector containing the set-exclusive-or values between the index vector [1…N] and the combination vector

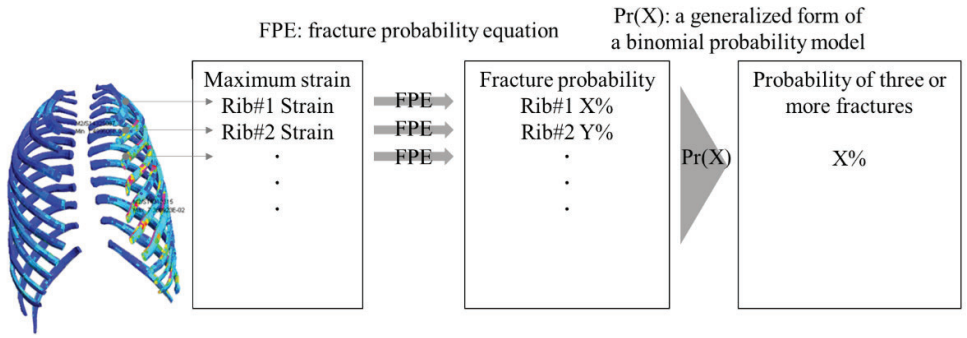

Figure 1: Probabilistic analysis

Evaluation of vHBM against thorax impactor tests

The vHBM was evaluated to compare the chest deflection in the thorax cylindrical impactor tests conducted by Talanikite et al. [13]. The vHBM was 3D scaled to two different subject body sizes (L02, L03) used in the experiment. The vHBM weight was also altered to match the mass of the two PMHS by adjusting the visceral density. The cylindrical impactor had a 15 cm diameter, a mass of 16 kg, and impacted the thorax of the subjects at a velocity of 6 m/s. The impact location to the vHBM was centered laterally on Rib 5 to match the experimental tests. Thoracic deflection was calculated from the impactor displacement relative to T8 and NHD was calculated by dividing the chest deflection by the chest width of the vHBM. Finally, the NHD from the simulated impacts was compared with the experimental results.

Evaluation of vHBM against realistic lateral sled tests

The vHBM was also evaluated using the sled tests with vehicle boundary conditions conducted by Shurtz et al. [6] and Bolte et al. [7]. As with the cylindrical impactor tests, the vHBM was used to reproduce the body size and mass of four of the PMHS used in the sled experiments by 3D scaling. Figure 2 shows the simulation model representing the vehicle-based sled tests, which included a mass-production seat, a three-point restraint with pretensioner, an intruding door liner, and an airbag. The ΔV applied to the simulated sled was the same as in the experiment at 28 km/h. The seatbelt pretensioner and airbag ignition timing were both set at 6 msec as in the physical experiment. The head block was modeled to mimic a foam block utilized in the lateral sled tests to represent a simplified side curtain airbag. The urethane foam had a strength of 0.15Mpa at 20% compression.

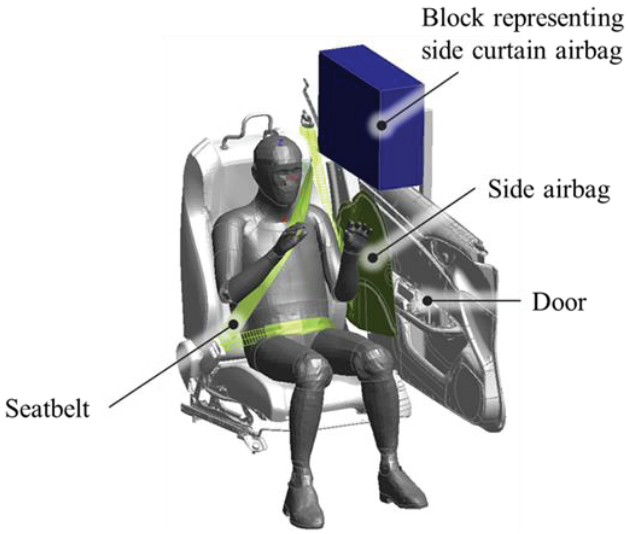

Figure 2: Configuration of vHBM simulation of realistic lateral sled tests

For this simulation NHD was measured at 50% of the ribs #5 and #6 at the mid-axillary line location similar to that in the experiment. The maximum principal strain on the rib cortical bone was calculated for each of the ribs 1-10 on the impact side. Using these maximum strains and the previously developed fracture probability equations, the probability of three or more fractures was calculated using the probabilistic analysis proposed by Forman et al. [12]. The upper and lower value of the NHD and the probability of rib fracture obtained from the simulation results were compared with the experimental data to verify the reproducibility of the injuries recorded in the PMHS sled tests.

Development of the injury prediction function (IPF) with additional simulations.

Since all of the experimental PMHS and simulation models reached AIS 3+, additional simulations were needed to identify cases where the number of rib fractures were reduced. Therefore, additional simulations were conducted with the simulated sled velocity at both 16 km/h and 24 km/h and also simulated with and without the airbag. All of the simulations were then combined to develop an IPF. The reduced values of ΔV correspond to published ΔVs with the highest frequency of AIS 2 and AIS 3 thoracic injury in accident data analysis for elderly female occupants in lateral crashes [14].

A total of 192 cases were simulated using 32 types of vHBMs (8 types of materials x 4 body sizes) in 6 different loading conditions (3 ΔVs, with and without airbag) to collect the data for an IPF. From the results of these simulations, the NHD at the mid-axillary line location for ribs #1 to #10 were measured. In addition, the maximum principal strain of each rib was measured and the probability of three or more fractures was calculated in each simulation case in the same way that was used for the evaluation of vHBM against the PMHS sled tests. The maximum NHD and the probabilistic analysis was plotted for the probability of three or more rib fractures, and the curve was fitted using logistic regression to develop the IPF with R software [15].

RESULTS

Development of Variability Human Body Model (vHBM)

Figure 3 shows the eight stress-strain curves for the material properties applied to vHBM. MAT124 PLASTICITY_COMPRESSION_TENSION in LS-DYNA was used for the cortical bone of the ribs. The range of the yield stress, elastic modulus and slope in the plastic region were 24-79 MPa, 7-15 GPa and 1.6-3.1 GPa, respectively (Table1). The material properties from subject 231 was the lower limit defined in this study.

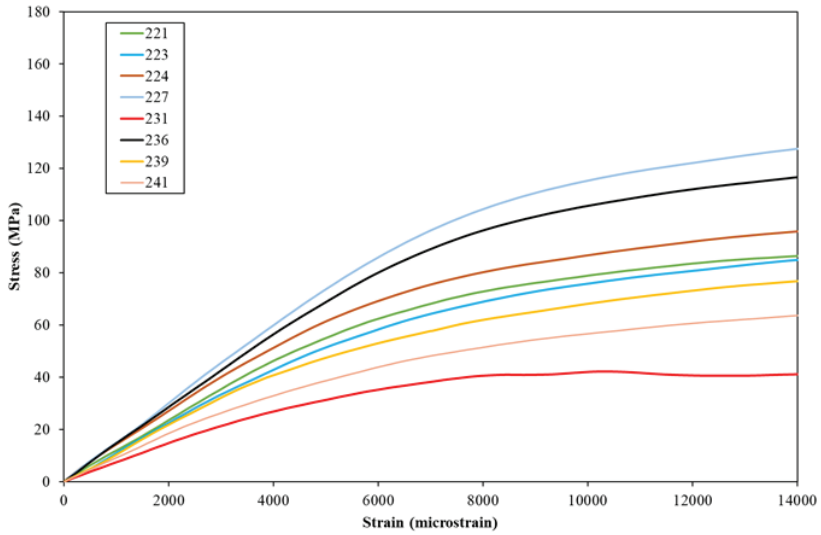

Figure 3: Rib cortical material for vHBM

Table 1: Rib cortical bone material properties

	221	223	224	227	231	236	239	241
Yield strain (10^{-6}):	4643	4643	4643	5313	3411	5852	3822	3260
Yield stress (MPa):	52	52	52	78	24	79	40	28
Elastic Modulus (GPa):	12	12	12	15	7	14	11	9
Slope in plastic region	2.8	2.8	2.8	3.1	1.6	2.7	2.8	1.9

The fracture probability equation was determined by fitting the test data using a survival analysis with Weibull distribution as shown in equation (2). Data were selected for ribs 1-7 from the literature with the age of 61 and above. The literature revealed that 50% of fracture probability was reached at 2.1% of strain. This fracture probability equation was applied to vHBM.

$$Fracture\ probability\ equation = 1 - exp\left(-\left(\frac{Strain}{2.430}\right)^{2.667}\right) \quad Equation\ (2)$$

Evaluation of vHBM against thorax impactor tests

Two simulations of the thorax impactor tests were conducted for the evaluation of vHBM. Chest deflection results are shown in Table 2. The maximum thoracic deflection differed with different cortical bone material parameters. The range of the maximum deflection in the LCT02 and LCT03 simulations were 0.28-0.31 and 0.22-0.27,

respectively. The change in the material parameters resulted in the change in the maximum deflection of approximately 15% for both subjects.

Table 2: Chest deflection of impactor simulation and experiment results

		LCT02	LCT03
Simulation	**221**	0.28	0.25
	223	0.28	0.24
	224	0.28	0.23
	227	0.27	0.23
	231	0.31	0.27
	236	0.28	0.23
	239	0.28	0.23
	241	0.29	0.22
	Range	0.27-0.31	0.22-0.27
Experiment		0.31	0.26

Evaluation of vHBM against sled tests

Injury reproducibility was verified under the PMHS lateral sled test condition with vehicle boundary conditions. In Table 3, NHD values are shown for both the simulation and experimental results. The range of deflection was 0.08-0.10, 0.11-0.13, 0.09-0.11 and 0.08-0.10 for Subject 1, 2, 3 and 5, respectively. The change in the material parameters resulted in the change in NHD by around 20% for all subjects. All but one of the simulations predicted 100% probability of AIS 3+.

Table 3: NHD of Sled simulation and experiment results

		Subject 1		Subject 2		Subject 3		Subject 5	
		NHD	**Probability of AIS3+**	**NHD**	**Probability of AIS3+**	**NHD**	**Probability of AIS3+**	**NHD**	**Probability of AIS3+**
Simulation	**221**	0.10	100%	0.11	100%	0.10	100%	0.09	100%
	223	0.10	100%	0.11	100%	0.10	100%	0.09	100%
	224	0.09	100%	0.11	100%	0.10	100%	0.09	100%
	227	0.08	100%	0.11	100%	0.09	100%	0.08	99%
	231	0.10	100%	0.13	100%	0.11	100%	0.10	100%
	236	0.10	100%	0.11	100%	0.10	100%	0.09	100%
	239	0.10	100%	0.12	100%	0.10	100%	0.09	100%
	241	0.10	100%	0.12	100%	0.11	100%	0.10	100%
	Range	0.08-0.10	100%	0.11-0.13	100%	0.09-0.11	100%	0.08-0.10	99%
Experiment		0.08	AIS3	0.13	AIS3	0.05	AIS3	0.09	AIS3

Development of the IPF with additional simulations.

The probability of three or more rib fractures and the maximum NHD results were plotted for all of the 192 simulations. The increase in NHD tended to increase the probability of three or more rib fractures as shown in Figure 4. The increase in NHD from 0.05 to 0.12 resulted in increase in fracture probability from approximately 20% and 80%, respectively. The IPF was formulated in Equation (3) by using logistic regression

$$Probability\ of\ AIS3+= \frac{e(-3.339 + 37.955 * NHD)}{1 + e(-3.339 + 37.955 * NHD)} \qquad Equation\ (3)$$

where NHD is maximum normalized half deflection.

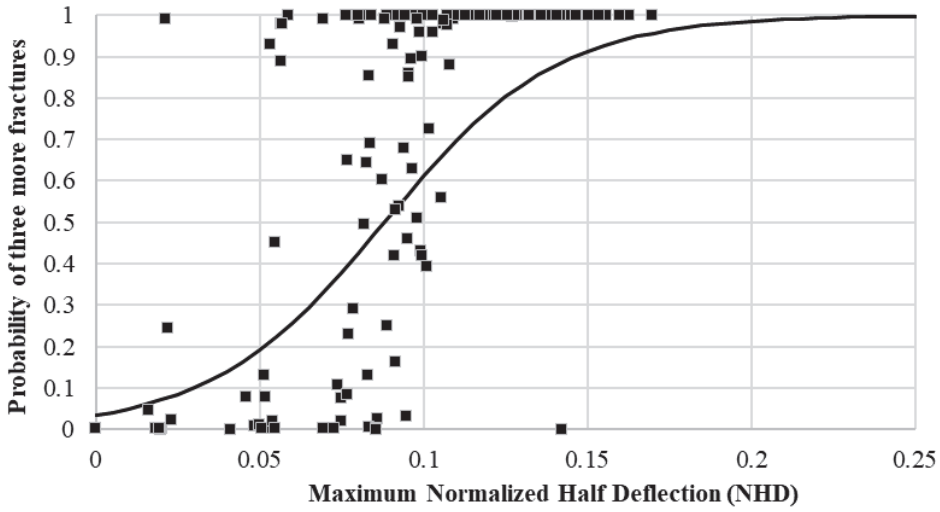

Figure 4: Probability of three or more fractured ribs

DISCUSSION & LIMITATION

The method of HBM

The experimental PMHS impactor and sled tests were reproduced by the vHBM simulations imparting individual variation in the material property of the cortical bone of the ribs. The experimental results fell within the range of the deflection obtained from the vHBM simulations that incorporated individual variability of the material property of the rib cortical bone, suggesting that the variability defined for the vHBM is a reasonable estimation of actual human variation. One exception was that the test results from one of the experimental PMHS subjects was not within the range of the variability predicted by the vHBM simulations. This may be due to the lack of consideration of other sources of variability, such as the thickness of the ribs or the geometry of the thoracic cage, which may be insufficient to reproduce variability in the material property of human bodies as indicated by Sugaya et al. [8] and Kang at al. [4]. Therefore, it may be necessary to further improve the reproducibility of individual variation in the future by reproducing other relevant sources of human variation.

Validity of IPF

Comparison of the IPF developed in this study with others in the literature showed an increased probability of three or more fractures. In addition, a comparison of the thoracic deflection from the PMHS sled tests and the fracture probability predicted by the parametric probability function showed that the IPF developed in this study was the closest to the IPF based on NHD and injury data from Bolte et al. [7] as shown in Figure 5. As a result, this probability function is likely to be reasonable under realistic vehicle boundary conditions.

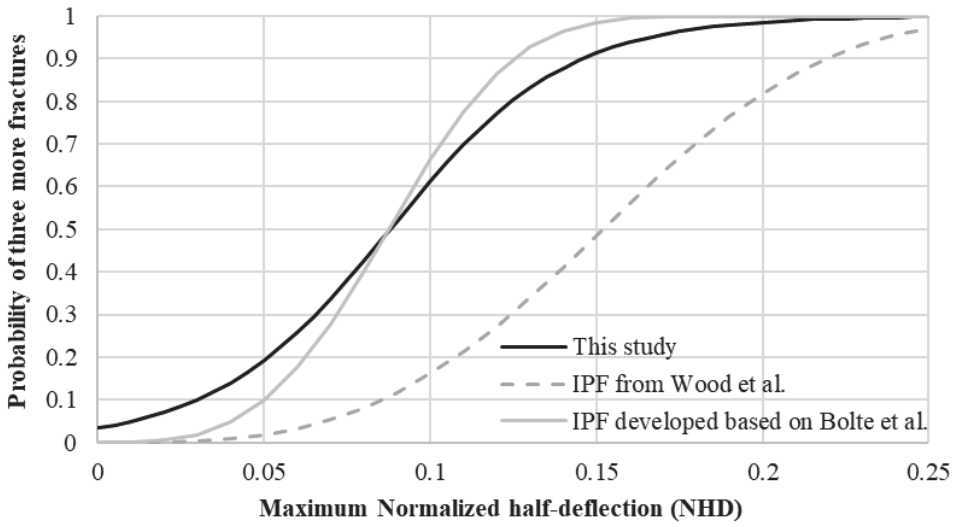

Figure 5: Probability of three or more fractured ribs comparing with literature

In the present IPF calculated by replicating the sled tests by Shurtz et al. [6] and Bolte et al. [7], differences in loading configurations may have influenced increased injury probability: the number of fractures increased in the elderly female due to pretensioning, or combined loading, as shown by Kawabuchi et al. [15]. The anterior-posterior deflection of the chest due to the activation of the pretensioner may have increased the strain in the ribs, and thus the influence of the seat belt, which was not seen in the impactor condition, may have been one of the factors contributing to the increased injury probability. It is possible that the combined loading of the lateral load from the airbags and the anterior-posterior load from the seatbelt may have increased the probability of injury. This suggests that injury probability depends on the loading configuration. Therefore, it is necessary to further improve the accuracy of the injury probability function by adding additional load cases in the future.

CONCLUSION

The vHBM was developed by applying material properties of rib cortical bone from a series elderly female coupon tests. The vHBM was able to predict chest deflections for both impactor and sled test configurations. An IPF was developed using the vHBM to represent the human variation under the boundary conditions of actual vehicles. The new IPF compared closely to the injury probability curve from the PMHS sled tests.

ACKNOWLEDGEMENT

The authors would like to gratefully acknowledge Dr. Andrew Kemper from Virginia Tech-Wake Forest University for providing their coupon test data for the rib cortical bone.

REFERENCES

[1] NHTSA-National Highway Traffic Safety Administration., 2022. “Overview of Motor Vehicle Crashes in 2020.” ,DOT HS 813 266: 4

[2] NHTSA-National Highway Traffic Safety Administration, 2005. “Characteristics of Crash Injuries among Young, Middle-Aged, and Older Drivers.”, DOT HS 810 857

[3] Ramachandra, R., Kashikar, T., Bolte, JH., 2017. “Injury Patterns of Elderly Occupants Involved in Side Crashes.”, The proceedings of International Research Council on Biomechanics of Injury (IRCOBI) Conference, 2017, Antwerp, Belgium.

[4] Kang, Y., Kwon, H., Stammen, J., Moorhouse, K., Agnew, M., 2020. “Biomechanical Response Targets of Adult Human Ribs in Frontal Impacts.”, Biomedical Engineering Society, 2021, Feb. vol 49

[5] Wood, L., Reed, M., Schneider, L., Klinich, K., Rupp, J., 2014. “Response and Tolerance of Female and/or Elderly PMHS to Lateral Impact.”, Stapp Car Crash Journal Vol 58, November 2014, San Diego, United States.

[6] Shurtz, B., Agnew, A., Kang, Y., and Bolte, J., 2018, "Application of Scaled Deflection Injury Criteria to Two Small, Fragile Females in Side Impact Motor Vehicle Crashes.", SAE Technical Paper, 2018, 2018-01-0542

[7] Bolte, J., Fibbi, C., Tesny, A., Kang, Y., Agnew, A., Shurtz, B., Pipkorn, B., Rhule, H., Moorhouse, K.,” Analysis of Injury Mechanism and Thoracic Response 1 of Elderly, Small Female PMHS in Near-Side Impact Scenarios.”, In Proceedings of 27th International Technical Conference on Enhanced Safety of Vehicles (ESV), 2023, Yokohama, Japan (to be published)

[8] Sugaya, H., Takahashi, Y., Gunji, Y., Dokko, Y., Ayyagari, M., Whitcomb, B., Markusic, C., Agnew, A., Kang, Y., Bolte, J., 2019. “DEVELOPMENT OF A HUMAN FE MODEL FOR ELDERLY FEMALE OCCUPANTS IN SIDE CRASHES.”, The Proceedings of 26th International Technical Conference on Enhanced Safety of Vehicles (ESV), 2019, Einthoven, Netherland

[9] LIVERMORE SOFTWARE TECHNOLOGY CORPORATION (LSTC), 2014. “LS-DYNA® KEYWORD USER'S MANUAL VOLUME II Material Models.”, LS-DYNA R7.1, May 19 2014: 632-635

[10] Katzenberger, M., Albert, D., Agnew, A., Kemper, A., 2020. “Effects of sex, age, and two loading rates on the tensile material properties of human rib cortical bone.”, Journal of the Mechanical Behavior of Biomedical Materials,2019, 102, August

[11] Kemper, A., McNally, C., Kennedy, E., Manoogian, S., Rath, A., Ng, T., Stitzel, J., Smith, E., Duma, S., Matsuoka, F., 2005. “Material Properties of Human Rib Cortical Bone from Dynamic Tension Coupon Testing.” ,Stapp Car Crash Journal, 2005, Vol.49, November: 199-230.

[12] Forman, J., Kent, R., Mroz, K., Pipkorn, B., Bostro, O., Gomez, M., 2012. “Predicting Rib Fracture Risk With Whole-Body Finite Element Models: Development and Preliminary Evaluation of a Probabilistic Analytical Framework.”, 56th AAAM Annual Conference Annals of Advances in Automotive Medicine, ,2012, October 14-17, Seattle, United States

[13] Talantikite, Y., Bouquet, R., Ramet, M., Guillemot, H., Robin, S., Voiglio, E., 1998. “Human Thorax Behaviour for Side Impact: Influence of Impact Masses and Velocities.” In Proceedings of International Technical Conference on the Enhanced Safety of Vehicles Conference (ESV), 1998, May31-June 4, Ontario, Canada

[14] Sugaya, H., Takahashi, Y., Ayyagari, M., Gomez, J., Whitcomb, B., Markusic, C., Ramachandra, R., Kang, Y., Agnew, A., Bolte, J., 2018.” Identification of Accident Representative Scenario for Elderly Female Occupants in Side Impact.” International Journal of Automotive Engineering, 2018: 150-155

[15] R Development Core Team, 2006, “R: A language and environment for statistical computing. Vienna (Austria): R Foundation for Statistical Computing.” Available: http://www.R-project.org/. , 2018, 30 June

APPENDIX A

TEST	ID	RIB #	Sex	Age	Fracture strain(ustrain)	strain(%)
Kemper et al.	Cad1-3L	3	F	64	36064	3.61
Kemper et al.	Cad1-3P	3	F	64	20789	2.08
Kemper et al.	Cad4-3A	3	F	61	35332	3.53
Kemper et al.	Cad4-3L	3	F	61	31069	3.11
Kemper et al.	Cad4-3P	3	F	61	25762	2.58
Kemper et al.	Cad1-4L	4	F	64	22208	2.22
Kemper et al.	Cad4-4A	4	F	61	36077	3.61
Kemper et al.	Cad4-4L	4	F	61	27386	2.74
Kemper et al.	Cad4-4P	4	F	61	16482	1.65
Kemper et al.	Cad1-5A	5	F	64	18404	1.84
Kemper et al.	Cad1-5L	5	F	64	11271	1.13
Kemper et al.	Cad4-5A	5	F	61	29876	2.99
Kemper et al.	Cad4-5L	5	F	61	21804	2.18
Kemper et al.	Cad1-6A	6	F	64	13471	1.35
Kemper et al.	Cad1-6L	6	F	64	27903	2.79
Kemper et al.	Cad4-6L	6	F	61	13519	1.35
Kemper et al.	Cad4-6P	6	F	61	26274	2.63
Kemper et al.	Cad1-7A	7	F	64	5217	0.52
Kemper et al.	Cad4-7A	7	F	61	45858	4.59
Kemper et al.	Cad4-7L	7	F	61	18873	1.89
Katzenberger et al.	261	6	F	93	10638	1.06
Katzenberger et al.	180	6	F	69	14499	1.45
Katzenberger et al.	103	6	F	75	9509	0.95
Katzenberger et al.	367	6	F	87	18196	1.82
Katzenberger et al.	363	6	F	87	14932	1.49
Katzenberger et al.	352	6	F	90	13110	1.31
Katzenberger et al.	221	6	F	74	19518	1.95
Katzenberger et al.	223	6	F	82	17353	1.74
Katzenberger et al.	224	6	F	76	24528	2.45
Katzenberger et al.	227	6	F	66	16364	1.64
Katzenberger et al.	231	6	F	92	14283	1.43
Katzenberger et al.	236	6	F	84	26115	2.61
Katzenberger et al.	239	6	F	70	19265	1.93
Katzenberger et al.	241	6	F	99	27825	2.78

PROBABILITY FUNCTIONAL EVALUATION OF CHEST INJURY BASED ON RIB STRAIN OF HUMAN BODY MODEL IN FRONTAL COLLISION

Yoshiki Takahira
Shizue Katsumata
Takeshi Yamamoto
Mitsutoshi Masuda
Toyota Motor Corporation
Japan

Paper Number 23-0218

ABSTRACT

This study examined the influence of chest restraint force on the chest injury probability of the human body model (HBM) in frontal collision. Total Human Model for Safety (THUMS) Version 4.1 AM50 was seated in the driver's seat of a finite element (FE) model represented a prototype midsize vehicle, and frontal collision simulations were performed. The probability of three or more rib fractures from 20YO to 80YO were predicted from simulated THUMS rib strain based on prior work. The probability increased with age, and showed a tendency to rise sharply beginning around the 60YO in particular. The trend was shown to be similar to the probability predicted statistically from the NASS-CDS field accident data. Furthermore, a collision simulation was also conducted in which the restraint balance between the seatbelt and airbag was changed while keeping the same amount of forward excursion of the occupant. As a result, it was found that the probability of rib fracture was reduced by the combination of reducing the seatbelt force and increasing the initial restraint force of the airbag compared to a base specification. This was due to the improved ride-down efficiency and reduced seatbelt contact force, which reduced the strain on the upper ribs on the path of seatbelt.

INTRODUCTION

Frontal collisions account for a high proportion of fatal crashes involving vehicle occupants. Chest injury is the most common cause of death and injury among belted occupants. It has been reported that the ribs deflect due to strong external force on the chest, causing pulmonary contusion and aortic injury [1]. In addition, if multiple ribs are fractured, normal chest wall function becomes difficult, which is called flail chest, and respiratory failure may occur. In recent years, CAE simulation using HBMs has been utilized to investigate the mechanism of chest injury and research safety technology. HBMs are modeled the geometry and characteristics of the human chest with reference to the anatomy. They have the advantage of being able to simulate the boney and organ strain. Kitagawa et al. evaluated the effects of four-point shoulder belts and air belts with THUMS Version 4 and Mroz et al. evaluated the effects of 3 + 2 criss-cross belts and split buckles with the Elderly THUMS TUC, using rib bone strain. However, most of HBMs refer to the shape data of a specific individual, and there is a large dependence on the model shape so even with the same body size. In addition, the stress-strain characteristics and bone thickness of ribs are greatly affected by individual differences and age differences [5-6], further complicating issues in quantitative injury evaluation with HBMs. Therefore, Forman et al. developed a methodology for predicting the probability of an arbitrary number of rib fractures from the rib strain of HBM using a probability function adjusted based on the results of thoracic impactors, seatbelt compressions, sled tests, etc. using Post Modern Human Subject (PMHS) [7-8]. It is expected that equivalent evaluation of chest injury probability will be possible even if different HBMs such as THUMS, The Global Human Body Models Consortium (GHBMC), and SAFER HBM are used.
In this study, CAE simulations were performed using the THUMS Version 4.1 AM50 occupant model to assume a frontal collision of a medium-sized vehicle, and the probability of three or more rib fractures was predicted based on the rib strain obtained by simulation. To validate the probability, results were compared

with the probability of 3 or more rib fractures in a medium-sized male in frontal collision calculated by Forman et al. using the NASS-CDS field accident database [8]. Furthermore, using this simulation model, the probability of chest injury was predicted for three different restraint balance patterns of seatbelts and airbags, and the factors that caused the difference in the injury probability due to the applied force to the chest were investigated.

METHOD

Frontal Collision Simulation

The simulations were performed using FE models. The LS-DYNATM Version 971 was used for the FE analysis solver developed by Ansys (US). The vehicle frontal collision simulations were performed using the THUMS Version 4.1 AM50 occupant model (Figure 1). The occupant model represents a medium-sized male occupant with a height of 178 cm and a weight of 75 kg, about 35 years old. The model describes the anatomical features of human body, including the major skeletal structure, articular ligaments, brain, internal organs and other soft tissues. THUMS' mechanical responses were validated for various loading cases using PMHS test data described in the literatures [9-11]. A FE model representing the driver's seat of a medium-sized car was used, and an acceleration pulse for a frontal collision was applied. The interior parts (steering, instrument panel, pedals, seats, seatbelt and airbags) that could come into contact with the occupants were assumed to be deformable, while the windshield and floor panel were assumed to be rigid. The seatbelt retractor model simulated the functions of a pre-tensioner and a load-limiter. The deployment of the driver airbag (DAB) and knee airbag (KAB) was also simulated. The occupant behavior in the simulation model is consistent with the result of sled test using PMHS conducted by Albert et al. [12-14].

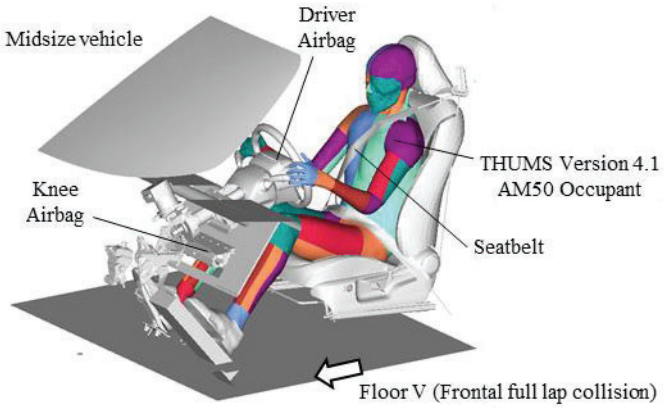

Figure 1. THUMS frontal collision simulation model

Simulation Matrix

A total of six simulations were conducted: two cases of speed change (delta V) of 40 km/h and 56 km/h; three cases of restraint system specifications with different restraint balances between seatbelt and DAB (Figure 2, 3, Table 1). A general seatbelt load limiter and DAB were utilized in Base. Spec. A reduced the load limiter by 25% compared to Base. Spec. B increased the deployment depth by 25% without increasing the volume of the DAB compared to Spec. A. The internal pressure was adjusted so that the amount of the chest forward excursion in a collision with delta V of 56 km/h was equivalent to Base. The specifications of these three types of restraint systems are for research only and do not represent the characteristics of actual products.

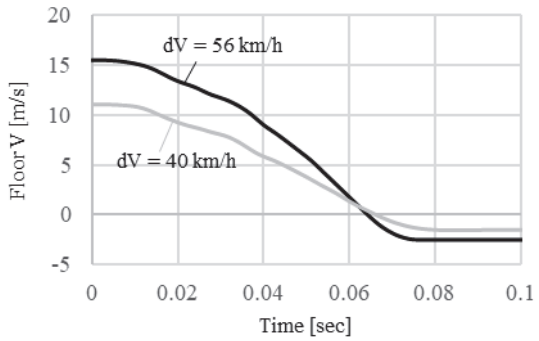

Figure 2. Time history of floor V in frontal full overlap collision

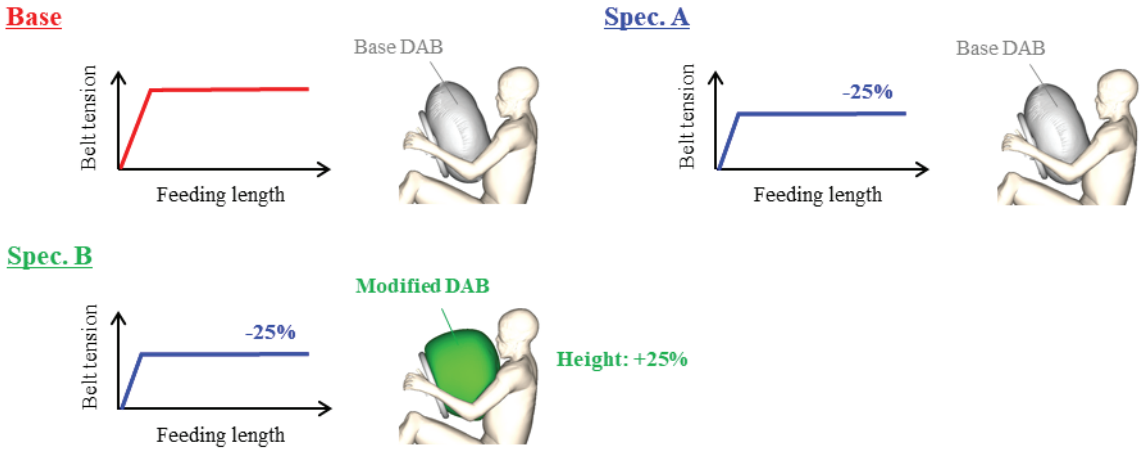

Figure 3. Specification of restraint system

Table 1.
Simulation matrix

Case	Delta V	Restraint system
#1	40 km/h	Base
#2	↑	Spec. A
#3	↑	Spec. B
#4	56 km/h	Base
#5	↑	Spec. A
#6	↑	Spec. B

Prediction of Chest Injury Probability by THUMS

The probability of three or more rib fractures (AIS3+) from the principal strain of the rib cortical bones obtained from the simulation was calculated using the chest injury probability function for THUMS proposed by Forman et al. (Figure 4). In this methodology, the fracture probability for each of the 12 left and right ribs is first obtained from the relationship between the principal strain 95tile (MPS95) of the ribs and the fracture probability adjusted based on the results of the PMHS tests. Next, the probability of any number of fractures is calculated using the generalized binomial model. An age term is included in this function, and with increasing age there is a higher probability of fracture at lower strains.

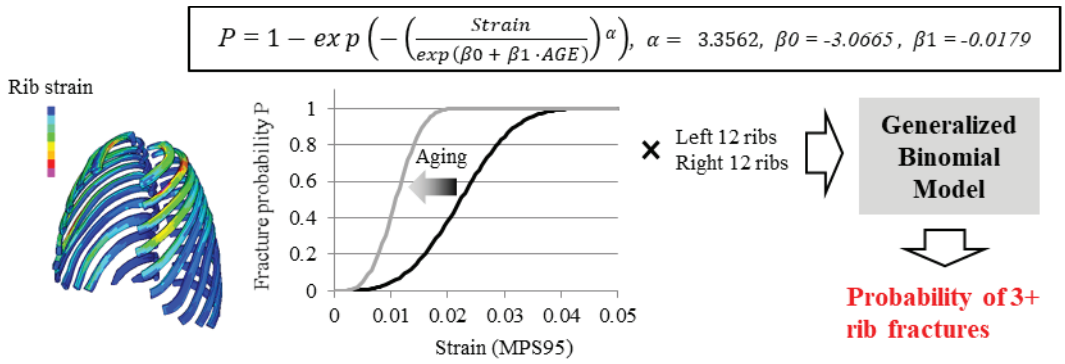

Figure 4. Chest injury probability function for THUMS V4.1 [8]

RESULTS

Occupant Kinematics

Figure 5 shows the occupant kinematics at maximum forward excursion of the chest. The numerical values in the figure represent the amount of chest (T4) excursion based on the floor. At delta V of 40 km/h, the chest excursion in base was 322 mm, while it increased to 351 mm with Spec. A, which has reduced belt tension compared to Base. Furthermore, that in Spec. B, which increased the deployment depth of the DAB compared to Spec. A, was 295 mm, which was 56 mm less than Spec. A. At delta V of 56 km/h, the amount of chest excursion in Base was 429 mm, while it increased to 466 mm with Spec. A. And that in Spec. B was 422 mm, 54 mm less than in Spec. A, which was the same as Base (as intended).

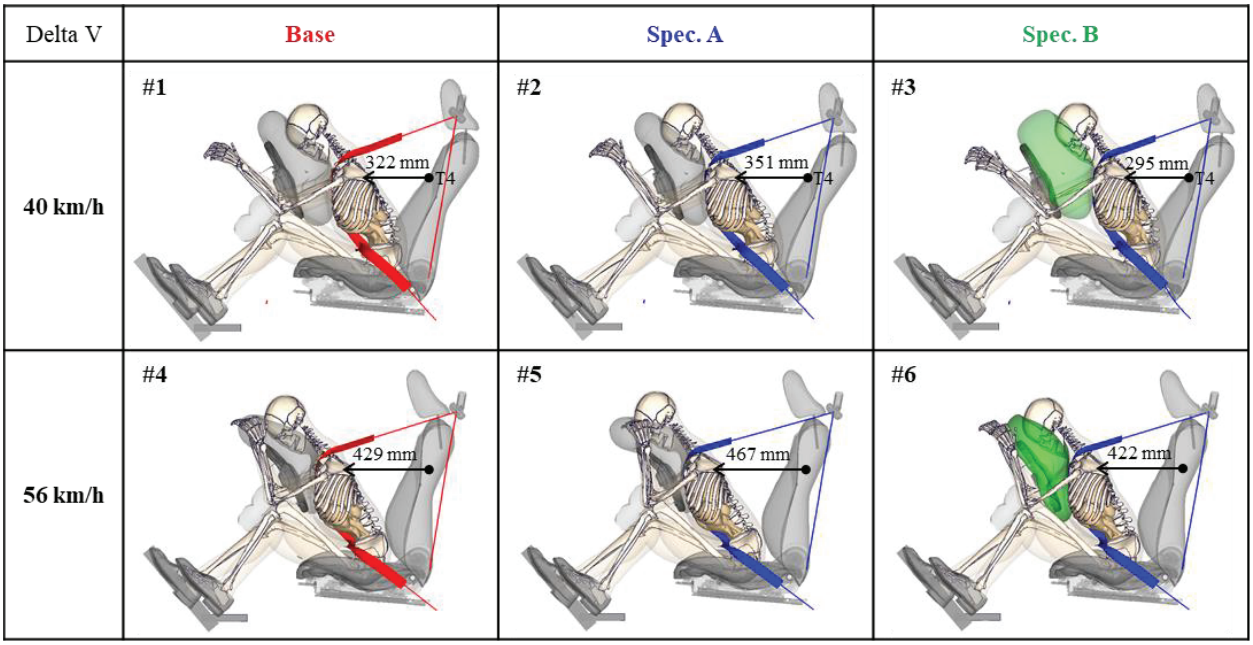

Figure 5. Occupant kinematics at maximum chest excursion

Applied Force to Anterior Chest

Figure 6 shows the force-stroke curve of the contact force applied to the anterior chest from the seatbelt and DAB and with respect to the amount of chest excursion. In Spec. A, which reduced the belt tension compared to Base, the belt contact force decreased from 5 kN to 4 kN, however the DAB contact force increased from

1.6 kN to 2 kN due to the increase in chest excursion. In addition, in Spec. B, which increased the DAB deployment depth compared to Spec. A, the amount of chest excursion decreased, but both the belt and DAB contact force were slightly reduced compared to Spec. A. At delta V of 56 km/h, Spec. A reduced the belt contact force from 6.4 kN to 5.2 kN compared to Base, however the DAB contact force increased from 3.5 kN to 4.2 kN. In Spec. B, the belt contact force decreased from 5.2 kN to 4.7 kN, and the DAB contact force decreased from 4.2 kN to 3.5 kN. compared to Spec. A.

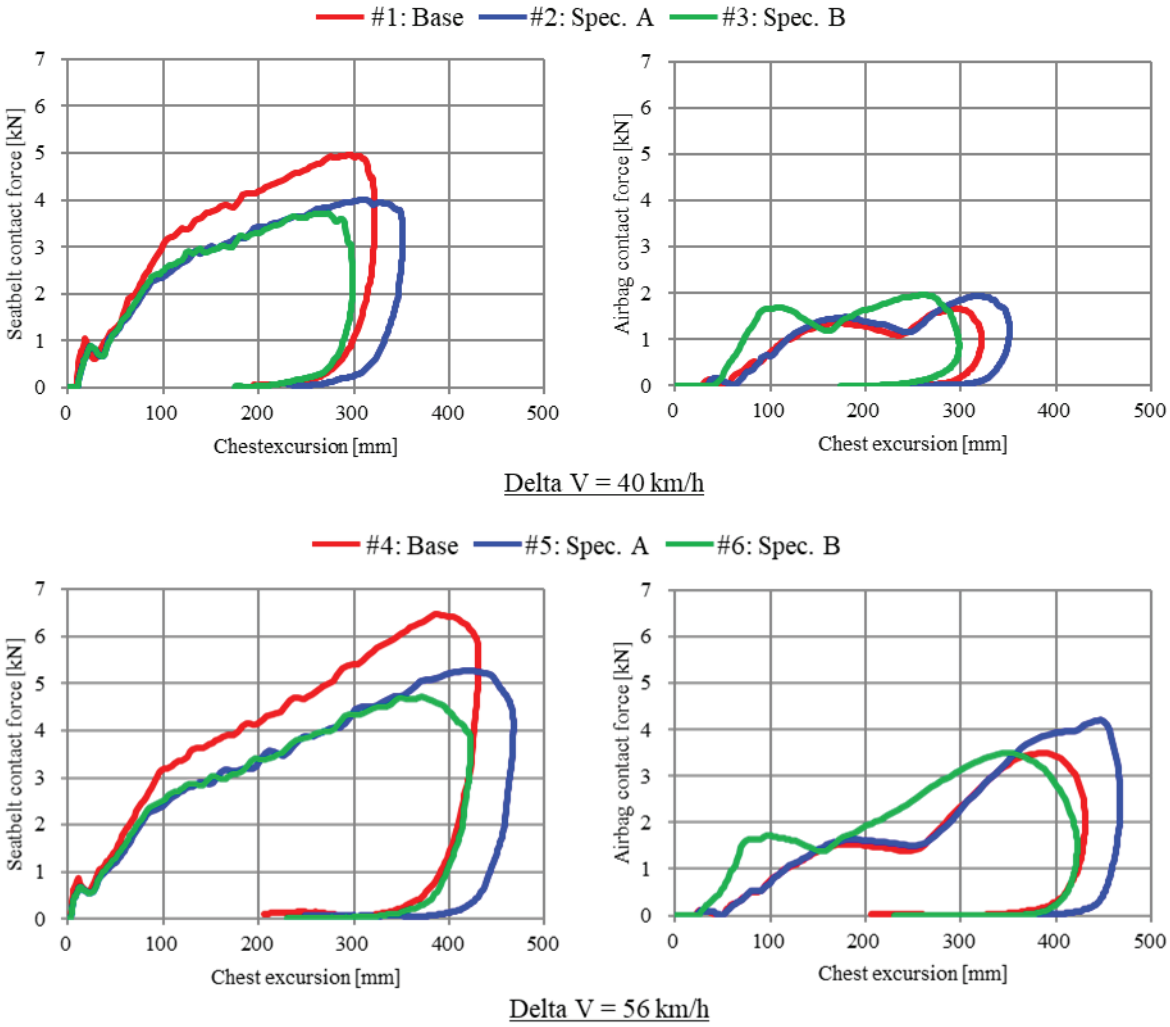

Figure 6. Chest applied force and excursion curve in CAE simulation

Rib Strain

Figure 7 shows the maximum principal strain distribution of the rib cortical bone, and Figure 8 shows the MPS95 of each ribs. In all cases, the left upper ribs, where the seatbelt was attached, tended to exhibit the most strain, and the strain level was generally higher at delta V = 56 km/h compared to delta V of 40 km/h. At delta V of 40 km/h, there was no difference in the strain level in all three cases. On the other hand, at delta V of 56 km/h, the strain level of Spec. A, which reduced the belt force, was the almost same as that of Base. However, in Spec. B, which had the higher deployment depth of the DAB, the amount of strain at left first rib was particularly reduced.

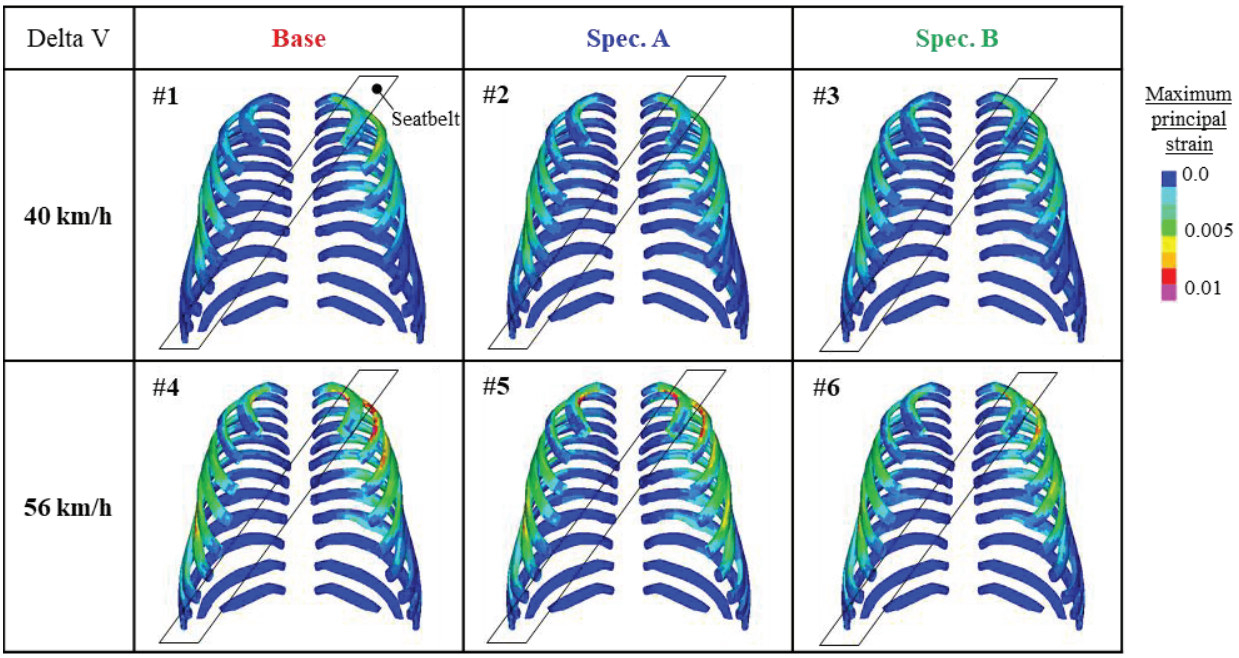

Figure 7. Maximum principal strain distribution rib cortical bones

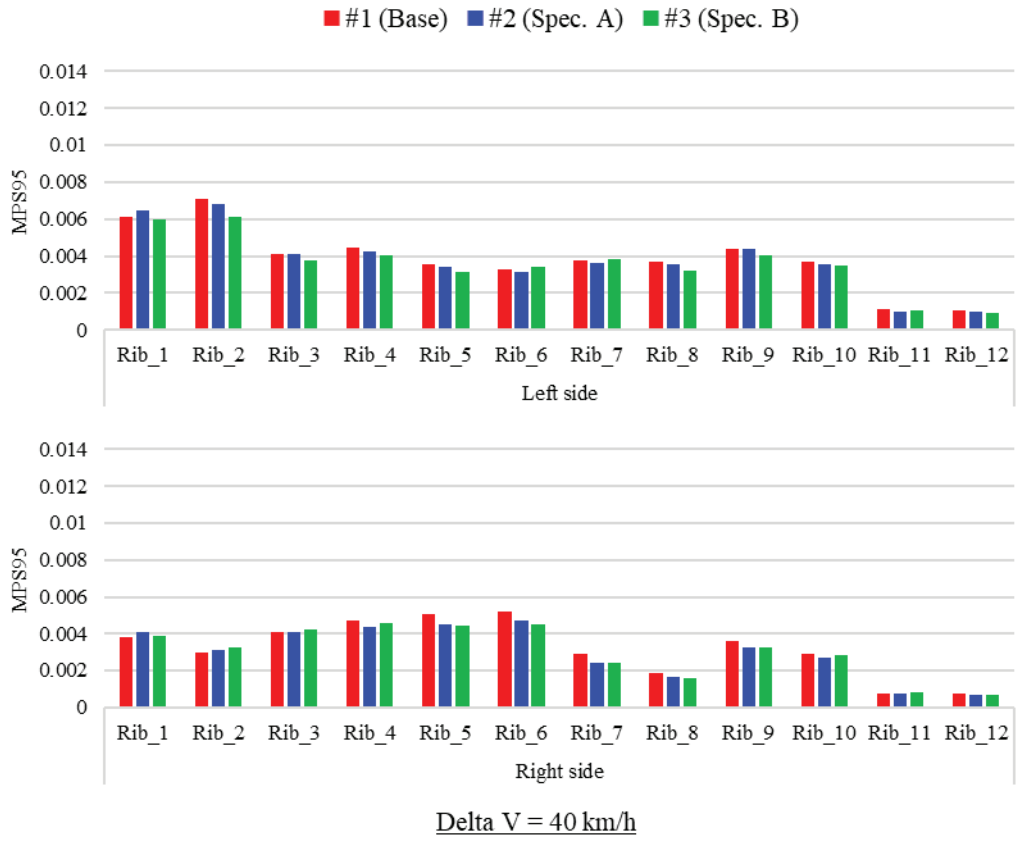

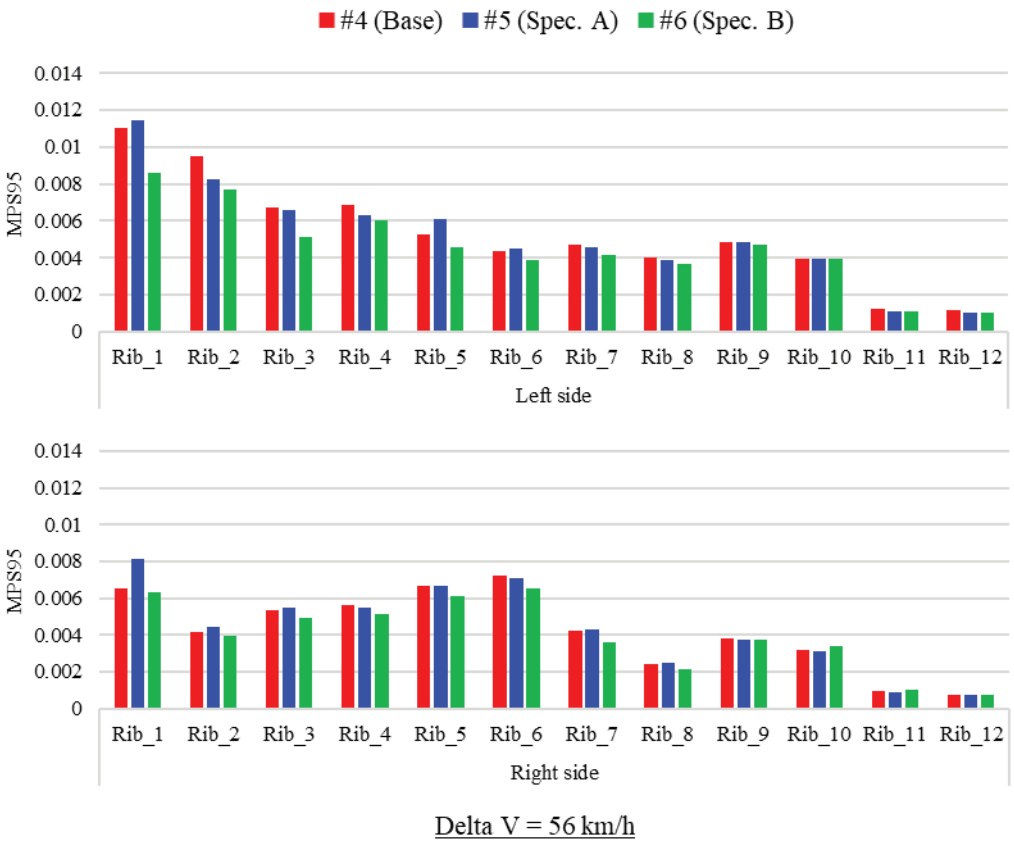

Figure 8. 95%tile of maximum principal strain(MPS95)

Chest Injury Probability

Figure 9 shows the probability of 3 or more rib fractures (AIS3+) calculated based on the rib strain obtained from the simulations. The horizontal axis represents the age of the occupant, and the vertical axis represents the probability. At delta V of 40km/h, the probability was almost 0 until 60YO and was below 5% even 80YO. On the other hand, at delta V of 56 km/h, the probability increased around 50YO, and it increased to nearly 20% at 70YO and to about 50% at 80YO in Base case. In addition, the probability of Spec. A with reduced belt force was almost same as Base regardless of age. Furthermore, the probability of Spec. B, which had the higher deployment depth of DAB, was reduced to about 5% at 70YO and about 25% at 80YO.

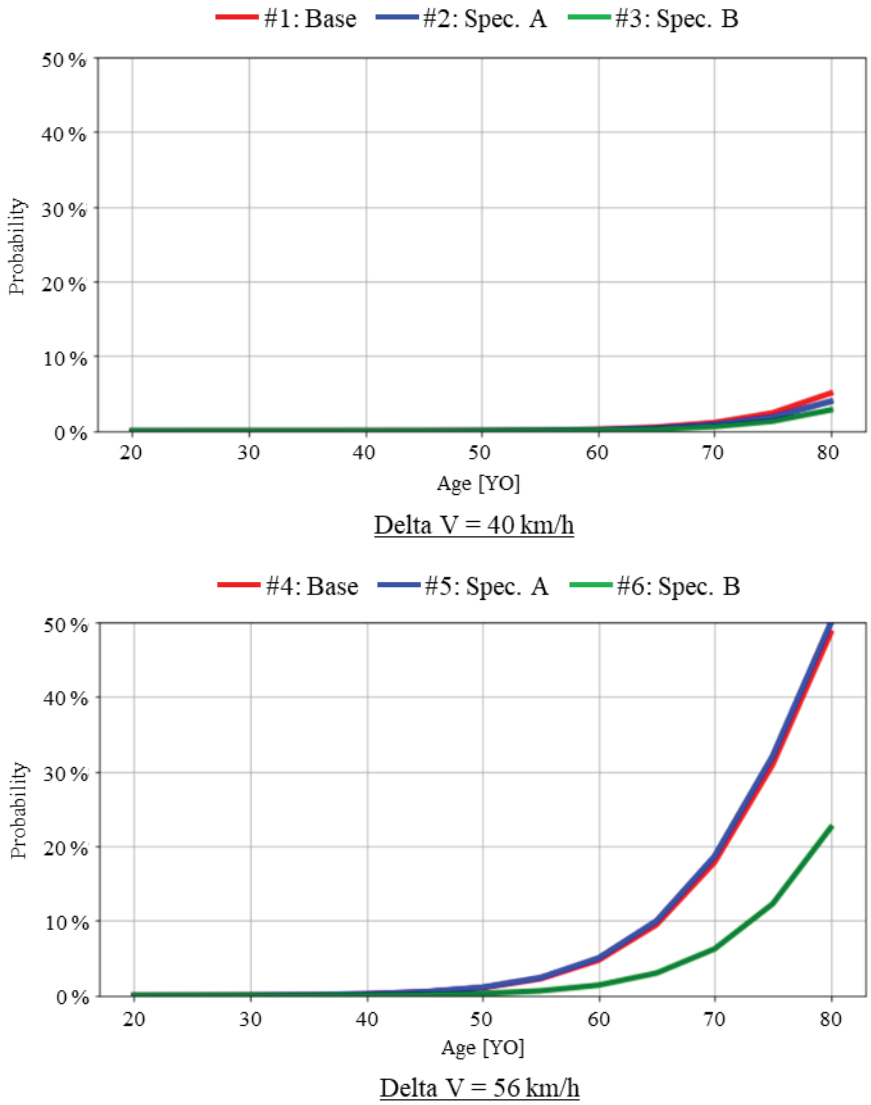

Figure 9. Probability of 3+ rib fractures

DISCUSSION

Validation of Chest Injury Probability of THUMS Simulation

Rib fracture probability calculated from the rib strain obtained in the frontal collision simulation using THUMS (#4) were compared with the probability statistically predicted from the NASS-CDS field crash database by Forman et al. [8] (Figure 10). Both results show the probability of 3 or more rib fractures for medium-sized male occupants aged 25, 45, and 65 in frontal collisions with delta V of 56 km/h. At the ages of 25 and 45, the simulation results were both less than 0.1%, and the results from crash data were 0.3% and 1.3%, respectively, both with probabilities close to zero. On the other hand, at 65YO, the simulation result increased to 9.5% and result from crash data increased to 6.2%, showing a similar trend.

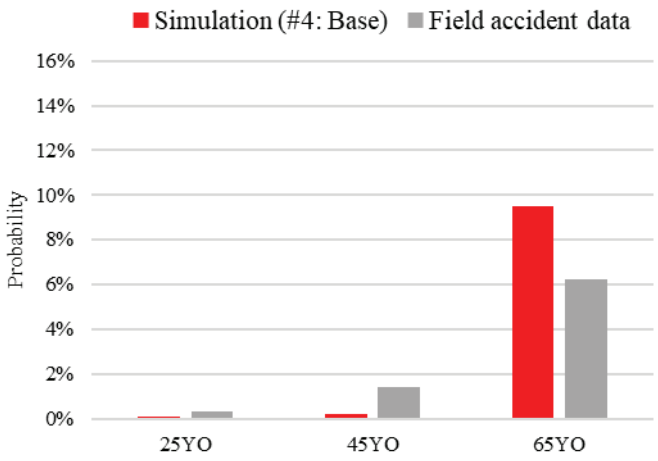

Figure 10. Probability of 3+ rib fractures in 56 km/h frontal collision

Influence of Restraint Balance on Chest Injury Probability

The probability of three or more rib fractures calculated from the rib strain distribution of THUMS was compared with three specifications with different restraint balances of the seatbelt and DAB. The left upper ribs, which exhibited the most strain, were deformed mainly by the clavicle intrusion due to the applied force from the seatbelt and airbag (Figure 11). At delta V of 56 km/h, no reduction in fracture probability was observed with Spec. A, which has a lower belt tension than Base. Although the applied force to the chest from the seatbelt decreased, the DAB reaction force increased due to the increase of chest excursion. As a result, the reduction of the total applied force to the chest was as small as 5% (Figure 12), with no reduction in the amount of clavicle deformation. In contract, in Spec. B, which combines a reduction in belt tension and an increase in DAB deployment depth, the fracture probability decrease by half. The increase in the initial restraint force of the DAB increased the ride-down efficiency and decreased the amount of chest excursion (Table 2). Therefore, both the seatbelt and DAB contact forces were reduced compared to Spec. A. As a result, the reduction rate of the total applied force to the chest compared to Base was as large as 18%, and the amount of clavicle deformation was reduced. It was indicated that a lower belt force is more effective in reducing the risk of rib fracture if the amount of chest excursion is similar.

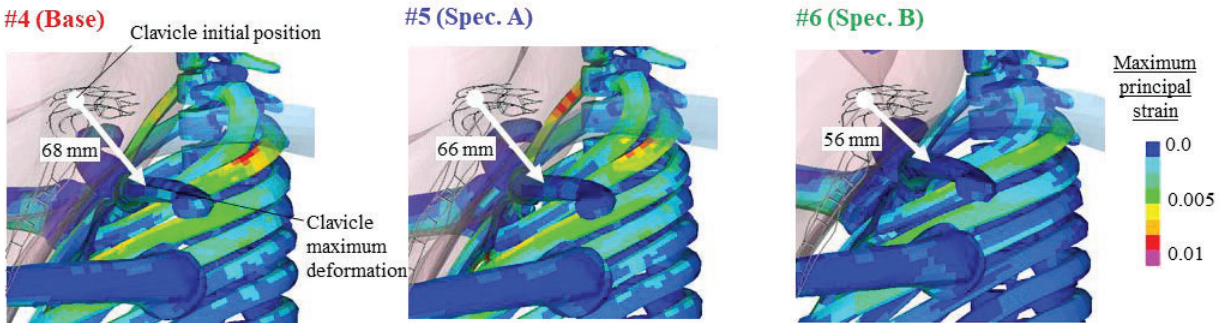

Figure 11. Deformed shape of scapula and upper ribs wrt. thoracic spine in 56 km/h frontal collision

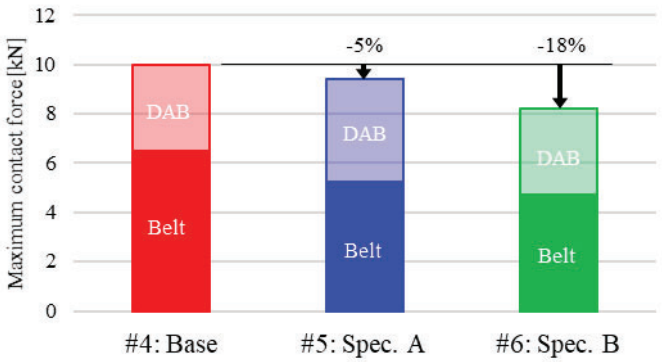

Figure 12. Maximum applied force to anterior chest in 56 km/h frontal collision

Table 2.
Ride-down efficiency of chest restraint in 56 km/h frontal collision

#4: Base	#5: Spec. A	#6: Spec. B
30.3%	25.4%	33.5%

LIMITATION

This study assumed a particular sitting posture and position for each occupant model, but of course this may vary among individuals and in specific situations. Interaction with restraint systems is also influenced by such factors. In addition, the prediction of rib fracture probability using field crash data includes various vehicle information, and of course it differs from the vehicle model used in this simulation, so further validations are necessary.

CONCLUSIONS

The rib fracture probability function proposed by Forman et al. was used to calculate the probability of three or more rib fractures, using the rib strain predicted by the frontal collision simulation using the THUMS Version 4.1 AM50 occupant model. Since the results showed a similar tendency to the prediction results of the field crash data, it was estimated that the prediction accuracy of the simulations were sufficient. Using this model, simulations with different restraint balances between seatbelt and DAB were performed. Compared to the base restraint system, the specification reducing only seatbelt force did not produce substantial reduction effect of the rib fracture probability. On the other hand, the specification that also included increasing the initial restraint force of the DAB to keep the same amount of chest forward excursion was effective in reducing the rib fracture probability. This study demonstrated the difference in rib fracture probability with different restraint systems, so this methodology is effective technology for future virtual assessment of crash safety.

REFERENCES

[1] Tominaga, S., Nishimoto, T., Motomura, T., Mashiko, K., Sakamoto, Y. 2012. “Analysis of Thoracoabdominal Injury based on Japan Trauma Data Bank and In-depth Accident Study.” Transactions of Society of Automotive Engineers of Japan, 43(2)

[2] Japanese Association for Acute Medicine. “Glossary of medical terms.” Internet: https://www.jaam.jp/dictionary/dictionary/word/0406.html

[3] Kitagawa, Y., Yasuki, T. 2013. “Correlation among Seatbelt Load, Chest Deflection, Rib Fracture and Internal Organ Strain in Frontal Collisions with Human Body Finite Element Models.” Proceedings of 2013 IRCOBI Conference

[4] Mroz, K., Pipkorn, B., Sunnevang, C., Eggers, A., & Brase, D. 2018. “Evaluation of Adaptive Belt Restraint Systems for the Protection of Elderly Occupants in Frontal Impacts.” Proceedings of 2018 IRCOBI Conference
[5] Courtney, C., Hayes, C., & Gibson, J. 1996. “Age-Related Differences in Post-Yield Damage in Human Cortical Bone. Experiment and Model.” Journal of Biomechanics, 29(11)
[6] McCalden, R. W., McGeough, J. A., Barker, M. B., & Court-Brown, C. M. 1993. “Age-Related Changes in The Tensile Properties of Cortical Bone. Journal of Bone and Joint Surgery.” 75-A
[7] Forman, J., Kent, Mroz, K., Pipkorn, B., Bostrom, O., Segui-Gomez, M. 2012. “Predicting Rib Fracture Risk with Whole-Body Finite Element Models: Development and Preliminary Evaluation of a Probabilistic Analytical Framework.” Proceedings of the 56th AAAM Annual Conference on Annuals of Advances in Automotive Medicine
[8] Forman, J., Kulkarni, S., Perez-Rapela, D., Mukherjee, S., Panzer, M., & Hallman, J. 2022. “A Method for Thoracic Injury Risk Function Development for Human Body Models.” Proceedings of 2022 IRCOBI Conference
[9] Watanabe, R., Miyazaki, H., Kitagawa, Y., & Yasuki, T. 2012. “Research of the relationship of pedestrian Injury to collision speed, car-type, impact location and pedestrian sizes using human FE model (THUMS Version 4).” Stapp Car Crash Journal, 561
[10] Shigeta, K., Kitagawa, Y., & Yasuki, T. 2009. “Development of next generation human FE model capable of organ injury prediction.” Proceedings of the 21st ESV Conference
[11] Kitagawa, Y., Hayashi, S., Yamada, K., & Gotoh, M. 2017. “Occupant kinematics in simulated autonomous driving vehicle collisions, direction and angle.” Stapp Car Crash Journal, 61
[12] Albert, D., Beeman, S., & Kemper, A. 2018. “Occupant kinematics of the Hybrid III, THOR-M, and postmortem human surrogates under various restraint conditions in full-scale frontal sled tests.” Traffic Injury Prevention, 19(S1)
[13] Albert, D., Beeman, S., & Kemper, A. 2018. “Assessment of Thoracic Response and Injury Risk Using the Hybrid III, THOR-M, and Post-Mortem Human Surrogates under Various Restraint Conditions in Full-Scale Frontal Sled Tests.” Stapp Car Crash Journal, 62
[14] Takahira, Y., Akima, S., Kusuhara, Y., Tanase, N., & Kitagawa, Y. 2021. “Cross-Sectional Analysis of Rib Fracture Mechanism of Elderly Occupant in Frontal Collision using THUMS.” Proceedings of 2021 IRCOBI Conference

METHODOLOGY TO PREDICT STRAIN OF BRIDGING VEIN DUE TO ROTATION OF HEAD

Yukou Takahashi
Toshiyuki Yanaoka
Honda R&D Co., Ltd.
Japan

Paper Number 23-0261

ABSTRACT

The brain stem can be damaged by the herniation of the brain tissue, potentially leading to fatality. Mass lesion could lead to fatality due to brain stem herniation, necessitating the prediction of the strain of the bridging veins (BVs). A number of trabecula forming a web-like structure of the sub-arachnoid space (SAS) may allow the assumption that the strain of the BVs correlates with that of the SAS. The objective of this study is to investigate the predictive capability of the strain in both the brain parenchyma (BP) and the SAS using a simplified physical model based on the CIBIC (Convolution of Impulse Response for Brain Injury Criterion) criterion proposed by the authors.

A viscoelastic model consisting of a series of two sets of standard linear solids (SLSs) used in the CIBIC criterion (extended version of CIBIC; e:CIBIC) was developed to represent both the BP and the SAS. The Global Human Body Models Consortium (GHBMC) head/brain model was used to obtain the target response of the maximum principal strain (MPS) in the BP and the SAS. Three angular acceleration time histories to be used to optimize model parameters were determined by combining twenty sine waves with the frequency ranging 10-200 Hz. The optimization of the spring and damping coefficients was performed by maximizing the CORA (CORrelation and Analysis) score for the time histories of the MPS in the BP and the SAS obtained from the GHBMC model. The optimized e:CIBIC was further assessed against a total of 256 sets of head rotational acceleration time histories obtained from frontal and side impacts and pedestrian impacts. The assessment was performed for the coefficient of determination of the correlation of the peak MPS with the GHBMC model along with the average value of the CORA score with the strain in both the BP and the SAS. The two assessment metrics were also compared against the original CIBIC criterion for the brain strain to clarify improved prediction.

The results of the performance assessment using the two metrics showed that e:CIBIC is capable of simulating the MPS in the BP with an accuracy similar to the original CIBIC. It was also found that the predictive capability of e:CIBIC for the MPS in the SAS is higher than that of the original CIBIC for the MPS in the BP.

This study revealed that e:CIBIC with the two sets of the SLS in series is capable of predicting the strain in both the SAS and the BP simultaneously. The results obtained in this study is dependent upon the validity of the head/brain FE model used. The relationship between the strain of the SAS and the probability of BV failure needs to be further investigated.

INTRODUCTION

Over the last couple of years, the number of traffic fatalities has decreased worldwide, largely due to the traffic volume drop coming from Covid-19 pandemic. According to the OECD report [1], the traffic volume dropped by 12.2% in 2020 compared to the average of 2017-2019 in 11 countries that collect data on travel volume. Consequently, the number of road death decreased by 8.6% across 34 member countries, with the majority of them seeing drop as much as 20%. Similar trend also applies specifically to Japan, with the reduction of the number of traffic fatalities of 18.4% among the same period [2]. Despite this significant decreasing trend in traffic fatalities, head injury is still responsible for the largest proportion in traffic fatality. Japanese accident statistics in 2021 [3] shows that the head accounts for 41.5% in the distribution of the major body part of the physical damage of all fatal accidents. It accounts for even more than half specifically in pedal cyclists (58.2%) and pedestrians (53.3%). Of those head injuries, traumatic brain injury (TBI) plays a significant role. Li et al. [4] reviewed 60 reports from 29 countries with data on TBI epidemiology and found that death was the most common outcome in patients with moderate and severe TBI. Motor vehicle collision (MVC) was the leading cause of TBI in 14 countries, including China, Japan, Australia, France, Spain, Austria,

Netherland and Italy. Such epidemiological findings have facilitated research aiming to establish a methodology to assess TBI in MVC.

In an effort to establish a methodology to assess TBI in MVC, Takahashi et al. [5] investigated the accident data from the National Automotive Sampling System (NASS) Crashworthiness Data System (CDS) from 2010 to 2014 and Pedestrian Crash Data Study (PCDS) from 1994 to 1998, with the head respectively comprising 33% and 46% of all body regions sustaining Maximum Abbreviated Injury Scale (MAIS) in fatal accidents. Of those head injuries, brain injury accounts for 78% and 81% of the head injuries responsible for the death for the data from NASS CDS and PCDS, respectively. Based on the tissue failure and anticipated injury mechanisms, types of TBI were classified into three major categories; pressure and/or skull fracture (brain contusion, epidural hematoma), brain strain (subarachnoid hemorrhage, intracranial hemorrhage and diffuse axonal injury) and displacement relative to the skull (subdural hematoma). The classification showed that TBIs primarily due to strain in the brain are by far most frequent, accounting for 81% and 73% of all TBIs for NASS CDS and PCDS database, respectively. Along with the early study by Holbourn et al. [6] that hypothesized that the shear strain in the brain primarily due to the rotational acceleration of the head is a predominant cause of brain damage due to large bulk modulus of the brain substance compared with its modulus of rigidity, many of recent studies have focused on the prediction of the strain in the brain primarily induced by head rotation in MVC.

In addition to the damage to the brain parenchyma (BP) due to the strain caused by the rotation of the head, the other important mechanism to consider is the rupture of the bridging vein (BV) that leads to acute subdural hematoma (ASDH). The rupture of the BV accumulates the blood between the dura mater and the cortex and generate hematoma that compresses the brain, which would lead very often to long term incapacity and high mortality rates [7]. Some of the studies have focused on detailed FE modeling of BVs to predict rupture of the BV [7][8] to enhance prediction capability of BV rupture. As currently available head/brain FE models generally use a set of simplified one-dimensional bar elements to represent the BVs [9], such detailed FE representation of the BVs would provide a valuable insight in the estimation of potential mechanism of BV rupture and subsequent ASDH. The other way to approach the issue, however, is to model the essential part of the physical phenomena involved in the mechanism of injury by means of a more simplified representation to provide a more practical means of injury assessment. The authors have applied this concept in the prediction of the strain in the BP to develop the CIBIC criterion [5]. It is based on the analytical solution of the response of the standard linear solid (SLS) model with a mass to acceleration time histories in three directions. The assumption was that the simplified viscoelastic model is capable of analogously representing the maximum principal strain (MPS) in the brain of the full-FE head/brain model with the brain tissue modeled using a linear viscoelastic material model. Surprisingly enough, good correlation was seen between the peak MPS predicted by the FE head/brain model and the CIBIC criterion. Subsequently, the same concept was also used by Gabler et al. [10], endorsing a good performance of such kinematics-based simple representation of the peak value of the MPS in the brain tissue. Although the validity of such simplified kinematics-based prediction models depend largely on the validity of the full-FE head/brain model against which model parameters are optimized, they still provide practical means of predicting brain response to impact based on the state-of-the-art prediction of brain injury mechanisms using full-FE simulations. However, to the best of the authors' knowledge, there has been no study that focuses on the prediction of BV rupture using a kinematics-based criterion.

The sub-arachnoid space (SAS) forms one of the three layers called the meninges that encase the brain and spinal cord. Anatomically, the SAS consists of a network of fine delicate connective tissue called sub-arachnoid trabeculae (SAT) that gives this space its characteristic spider web appearance. The SAT act as supportive pillars, allowing the flow of CSF [11]. SAT enclose the small blood vessels and adhere to the surface of larger blood vessels in the SAS and cisterns, providing mechanical support to neurovascular structures through cell-to-cell interconnections and specific junctions between the pia and arachnoid matters [12]. Such anatomical and clinical findings would lead to the assumption that the failure of the BV that goes though the SAS is related to the strain of the SAS in consideration of a simplified and kinematics-based prediction methodology of ASDH.

The goal of this study was to develop a methodology to predict rupture of the BV using a kinematics-based criterion. As the first step toward this ultimate goal, the current study focused on predicting the strain in the SAS along with the

prediction of the strain in the BP by means of extending the function of the CIBIC criterion to develop an extended version of the CIBIC criterion (e:CIBIC).

METHODS

e:CIBIC was developed by adding another set of the SLS in series to the single SLS used for the CIBIC criterion [5] to predict MPS in both the BP and the SAS simultaneously. The model parameters were determined using simplified rotational acceleration time histories to match the MPS in the BP and the SAS predicted by a full-FE 3D head/brain model. Similar to the CIBIC criterion, the numerical computation of e:CIBIC was replaced by the convolution integral to make sure that it yields the same results with a more simple calculation suitable for practical use. Finally, e:CIBIC expressed by the convolution integral procedure was validated against the same FE head/brain model in a number of crash test and simulation results.

Determination of model parameters

Figure 1 shows the comparison of the SLS model used for the CIBIC and e:CIBIC criterion for one particular direction of motion. e:CIBIC incorporates two sets of the SLS model each representing the BP and the SAS. As the lumped mass primarily represents the mass of the brain, and the rotational motion of the skull and the mandible is supposed to be given to the bottom of the lower SLS, displacement Xb and Xs respectively represent the strain in the BP and the SAS. Similar to CIBIC, the mass was set at 1.0 kg for simplicity and the model parameters were determined such that Xb and Xs predict the MPS in the BP and the SAS of the FE head/brain model. The model parameters determined included K_{b0}, K_{b1}, K_{s0}, K_{s1}, C_{b1} and C_{s1} (Figure 1).

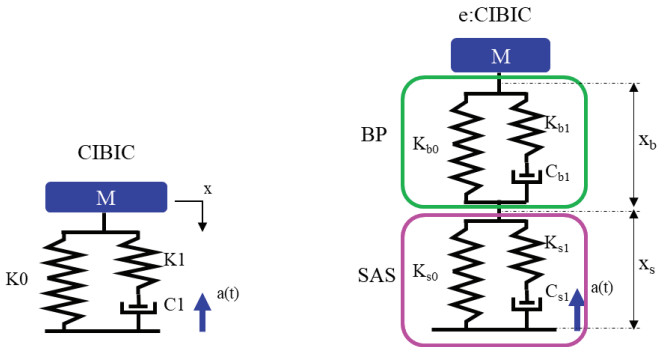

Figure 1. Comparison of the linear viscoelastic model used for CIBIC and e:CIBIC

Simplified rotational acceleration time histories were determined from actual impact test results to eliminate abnormal wave profiles. Ten full-frontal impact tests and ten moving deformable barrier side impact tests, each five of them coming from the largest and smallest peak head rotational acceleration groups, were chosen from the NHTSA vehicle crash test database [13]. In addition, ten car-pedestrian impact simulations were taken from those used in our previous study [5], each five of them coming from each of the largest and smallest peak head rotational acceleration groups. For all of these three impact configurations, the peak values were determined by the maximum of the three peak values in three rotational axes. The resulting thirty time histories were subjected to fast Fourier transform to determine distribution of the frequency and the amplitude. The frequency range was determined from the overall maximum and minimum value of the frequency range of each of the time histories determined between 90% and 100% of the maximum amplitude. The peak rotational acceleration was set at 5000 rad/s^2 by referring to the average value of the time histories used for the validation of the e:CIBIC in a later step. Three different simplified time histories were determined such that 1. the amplitude is the same for the entire frequency range, 2. the amplitude at the minimum frequency is ten times as much as the amplitude at the maximum frequency and 3. the amplitude at the maximum frequency is ten times as much as the amplitude at the minimum frequency (Figure 2). The resulting simplified rotational acceleration time histories are presented in Figure 3. These three simplified load cases are denoted as SLC 1 through 3.

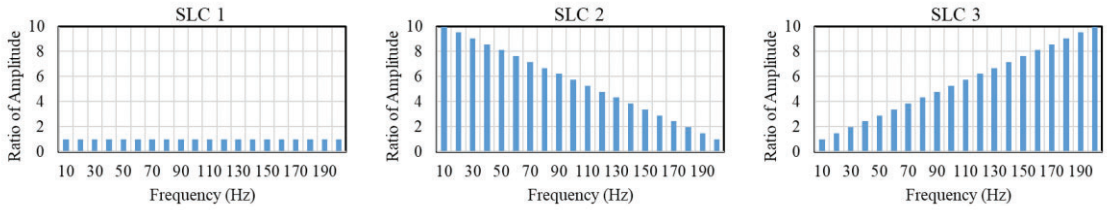

Figure 2. Distribution of amplitude by frequency

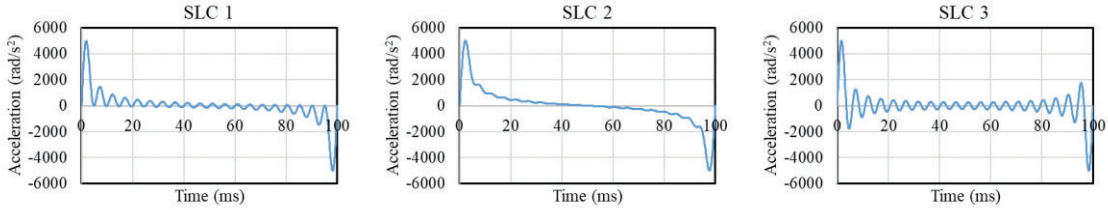

Figure 3. Simplified rotational acceleration time histories

These time histories were applied to both the e:CIBIC and the Global Human Body Models Consortium (GHBMC) head/brain model [9]. Rigid constraint was applied to the skull, mandible and flesh/skin of the GHBMC head/brain model with the prescribed acceleration time history applied to each of the three rotational axes (Figure 4). The rotational axes defined for this study are also illustrated in the figure. A numeric computing platform (MATLAB [14]) was controlled by an optimization software package (modeFRONTIER [15]) to optimize the model parameters of e:CIBIC using the optimization algorithm of MOGA-II. Due to the difference in the dimension of the MPS predicted by the FE head/brain model and X_b and X_s predicted by e:CIBIC, the time histories were normalized by their peak values and used for the optimization. Optimization was performed such that the summation of the CORA (CORrelation and Analysis) metric defined by the ISO/TS18571 [16] calculated for each of the six combinations of the three simplified rotational acceleration time histories and the two injury metrics (MPS in the BP and the SAS) is maximized for the normalized time histories. In addition to the determination of the model parameters, scaling factors S_b and S_s were determined to allow estimation of the MPS predicted by the FE head/brain model from the displacement calculated by the e:CIBIC criterion by dividing the peak value of the MPS from the FE head/brain model by the peak value of the displacement from the e:CIBIC criterion. The scaling factors were determined for each of the three simplified load cases and averaged to determine the final values to be used with the e:CIBIC criterion.

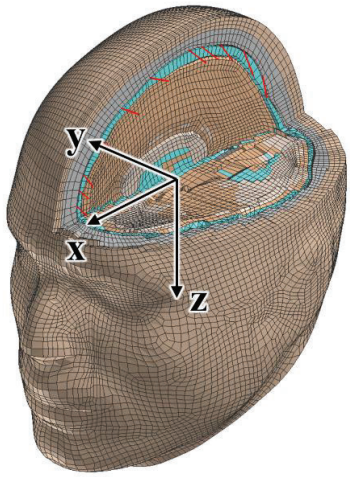

Figure 4. Schematic of the GHBMC head/brain model

Application of convolution integral

The convolution integral originally used to calculate the CIBIC criterion was applied to the calculation of the e:CIBIC criterion. The previous study to develop the CIBIC criterion [5] has found that in the current application, an impulse response can be well represented by the response to the step function with 1 ms duration. For this reason, the response of the e:CIBIC criterion to the step function with 1 ms duration was calculated for each of the three axes using MATLAB. Then the response in each of the three axes obtained was used to calculate e:CIBIC for a given rotational acceleration time history by means of the convolution integral. The e:CIBIC criterion is now defined using the following equations:

$$MPS_{BP} = S_b \sqrt{\sum_{i=1}^{3} \left\{ \int_0^t X_{bi}(t-\tau)\alpha_i(\tau)d\tau \right\}^2} \Bigg|_{max} \quad \text{Equation (1)}$$

$$MPS_{SAS} = S_s \sqrt{\sum_{i=1}^{3} \left\{ \int_0^t X_{si}(t-\tau)\alpha_i(\tau)d\tau \right\}^2} \Bigg|_{max} \quad \text{Equation (2)}$$

where MPS_{BP} and MPS_{SAS} denote the MPS in the BP and the SAS, respectively, S_b and S_s denote the scaling factor for the BP and the SAS, respectively, X_b and X_s denote the impulse response of the MPS in the BP and the SAS, respectively, α denotes the rotational acceleration, and $i = 1, 2, 3$ represent the x, y and z axis. The calculation was performed for the three simplified rotational acceleration time histories used to determine the model parameters to compare against the time history of e:CIBIC obtained by mean of MATLAB computation to make sure that the convolution integral used for the CIBIC criterion also works with the e:CIBIC criterion.

Validation

The model parameters determined for e:CIBIC were validated against the same GHBMC head/brain model in a number of different load cases in terms of both the correlation of peak values and the representation of time histories for the MPS in the BP and the SAS predicted by the GHBMC model.

The acceleration time histories of the head from the crash tests and simulations were prepared for the validation of the model parameters. ISO/TR19222 [17] assessed a number of different head injury metrics to predict the MPS in the brain subjected to rotational acceleration using the load cases from a variety of data sources. Of those, 71 full-frontal, 49 oblique frontal and 64 moving deformable barrier side impact tests that are currently available in the NHTSA database [13] were used. In addition, 62 pedestrian impact simulations performed by Takahashi et al. [5] were also referred to, resulting in 246 sets of head acceleration time histories in total. The crash tests and simulations used to determine the simplified head rotational acceleration time histories to determine model parameters were not included in the validation load cases.

Using the 246 load cases, the peak values of the MPS in the BP were plotted between the GHBMC head/brain model and the CIBIC criterion, and between the GHBMC head/brain model and the e:CIBIC criterion, respectively. Similarly, the peak values of the MPS in the SAS were plotted between the GHBMC head/brain model and the e:CIBIC criterion. The coefficient of determination (R^2) was calculated for each of the three plots to evaluate prediction capability of the e:CIBIC criterion relative to the 3D head/brain model and the CIBIC criterion. In addition, the CORA metric defined by ISO/TS18571 [16] was calculated for each of the 246 sets of the head rotational acceleration time histories between the GHBMC model and each of the CIBIC and the e:CIBIC criterion for the time history of the MPS in the BP, and between the GHBMC model and the e:CIBIC criterion for the time history of the MPS in the SAS. For each of the prediction models and the strain measure, the CORA scores obtained was averaged over all the load cases included in each of the four loading configurations (full-frontal, oblique-frontal, moving deformable barrier side and pedestrian impacts), as well as the grand total of 246 load cases and compared to each other to further validate the prediction capability of the e:CIBIC criterion.

RESULTS

Determination of model parameters

Figures 5 and 6 respectively compare the time histories of the MPS in the BP and the MPS in the SAS for the three rotational axes and the three simplified head acceleration time histories. The solid and the dotted curve represent the results from the e:CIBIC criterion and the GHBMC model, respectively. The six model parameters determined for the e:CIBIC criterion by averaging the optimized values over the three different simplified acceleration time histories are summarized in Table 1.

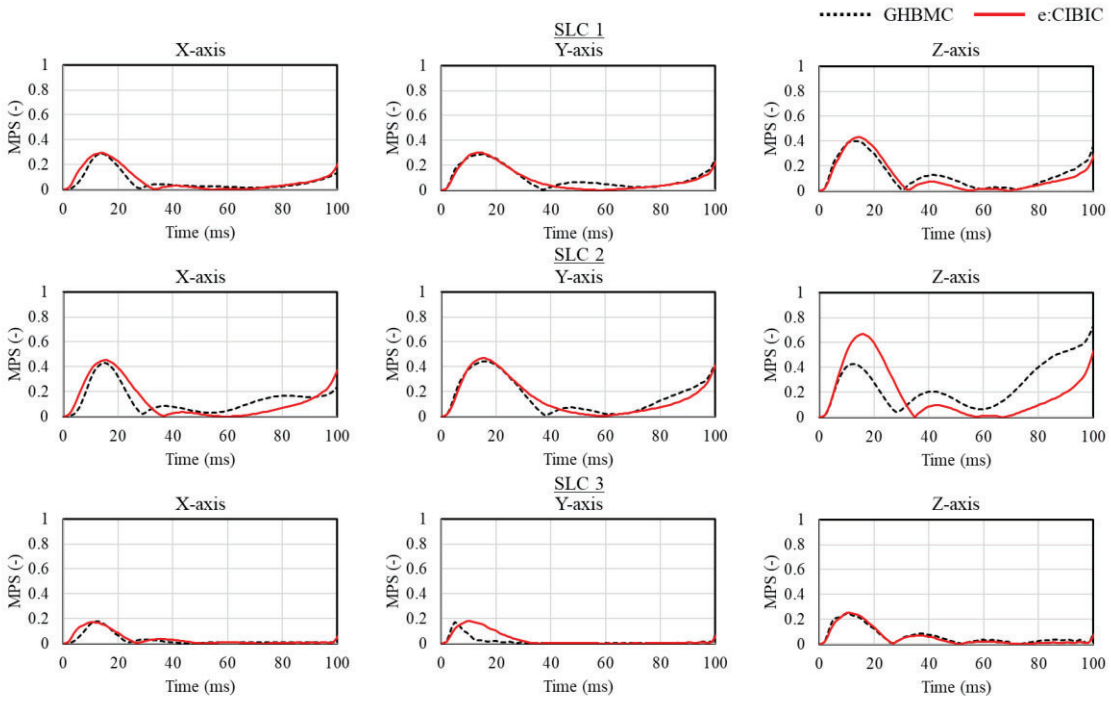

Figure 5. Comparison of the time history of the MPS in the BP between the GHBMC model and e:CIBIC

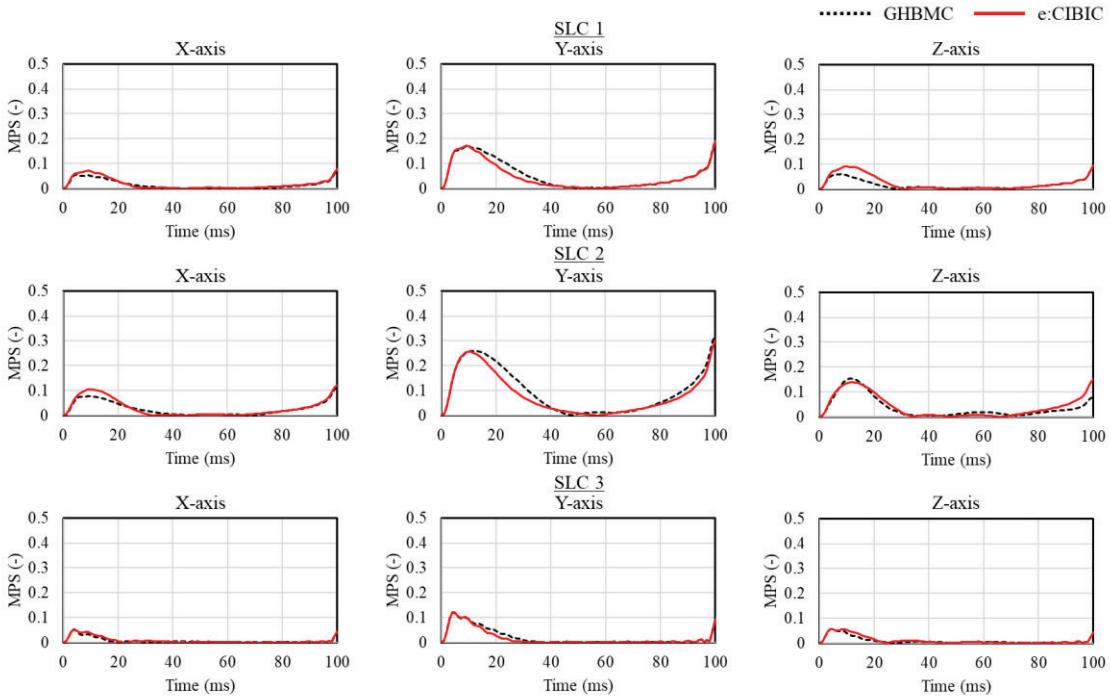

Figure 6. Comparison of the time history of the MPS in the SAS between the GHBMC model and e:CIBIC

Table 1.
Model parameters and scaling factors for e:CIBIC

Axis	K_{b0} (N/m)	K_{b1} (N/m)	C_{b1} (Ns/m)	K_{s0} (N/m)	K_{s1} (N/m)	C_{s1} (Ns/m)	Scaling Factor for BP	Scaling Factor for SAS
X	2.03E+04	1.46E+06	1.27E+02	2.82E+05	1.22E+05	1.83E+03	4.47	1.44E+01
Y	1.86E+04	4.99E+05	1.96E+02	1.31E+05	1.82E+05	9.98E+02	5.49	1.94E+01
Z	1.97E+04	6.36E+05	1.08E+02	1.69E+05	1.14E+05	1.24E+03	6.06	1.44E+01

Application of convolution integral

Figure 7 shows the time histories of the impulse response for both the MPS in the BP and the MPS in the SAS for x, y and z axis represented by the response to the 1 ms duration step function of the rotational acceleration time histories with the magnitude of 1.0 rad/s^2. Figure 8 presents the comparison of the time histories of the MPS in the BP and the SAS between the e:CIBIC criterion calculated using the convolution integral and the e:CIBIC calculated using MATLAB for the three simplified head acceleration time histories. The solid and dotted curves respectively represent the convolution integral and MATLAB calculation. The time histories are plotted for the resultant of the three axes.

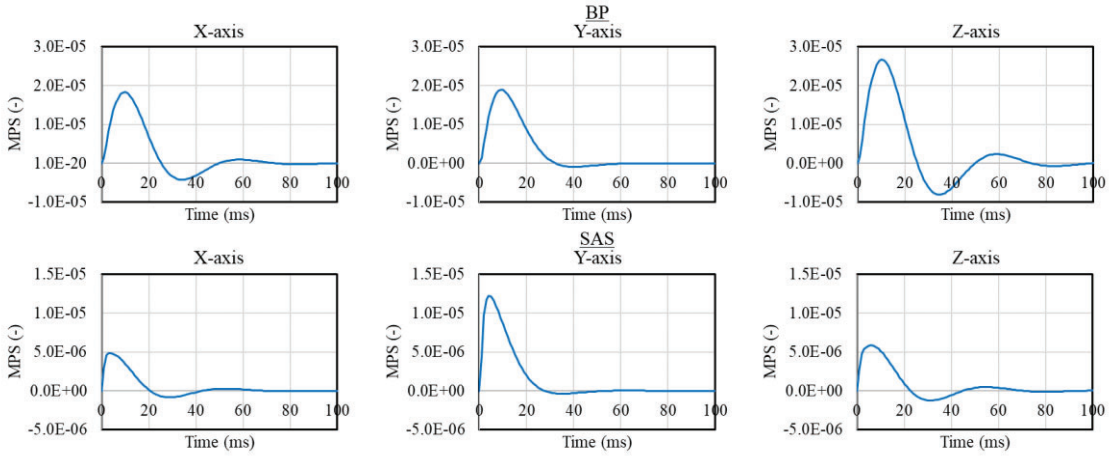

Figure 7. Impulse response of the MPS in the BP and the MPS in the SAS

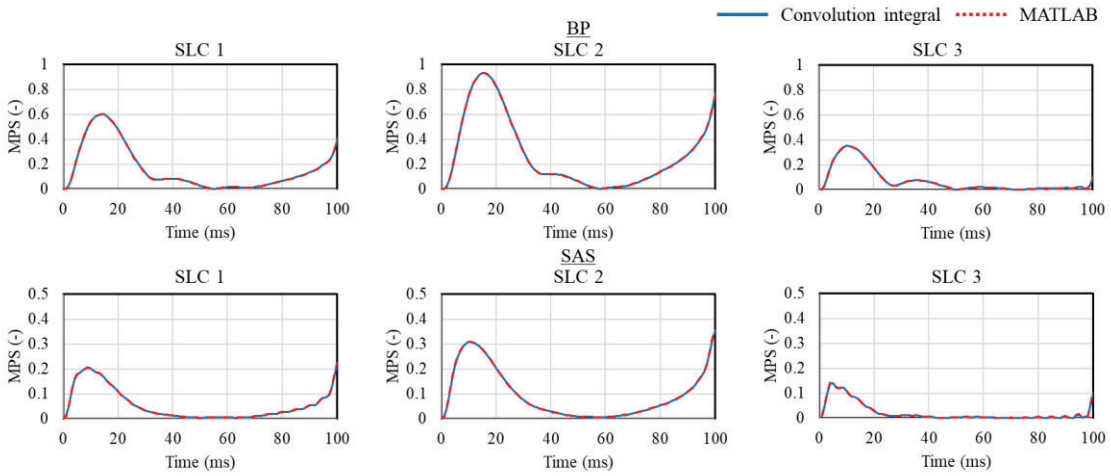

Figure 8. Comparison of the time history of the MPS in the BP and the SAS calculated using convolution integral and MATLAB

Validation

Figure 9 plots the correlation of the peak resultant values of the MPS for the load cases used for the validation. As for the MPS in the BP, the results obtained from the GHBMC model is plotted against both the CIBIC criterion and the e:CIBIC criterion, while the GHBMC model results are plotted only against the e:CIBIC for the MPS in the SAS due to the lack of prediction of the MPS in the SAS with the CIBIC criterion. Comparisons were made for all of the 246 load cases used, along with each one of the four impact configurations (full-frontal, oblique-frontal, moving deformable barrier side and pedestrian impact). Table 2 summarizes the coefficient of determination (R^2) obtained from each of the correlation plots presented in Figure 9.

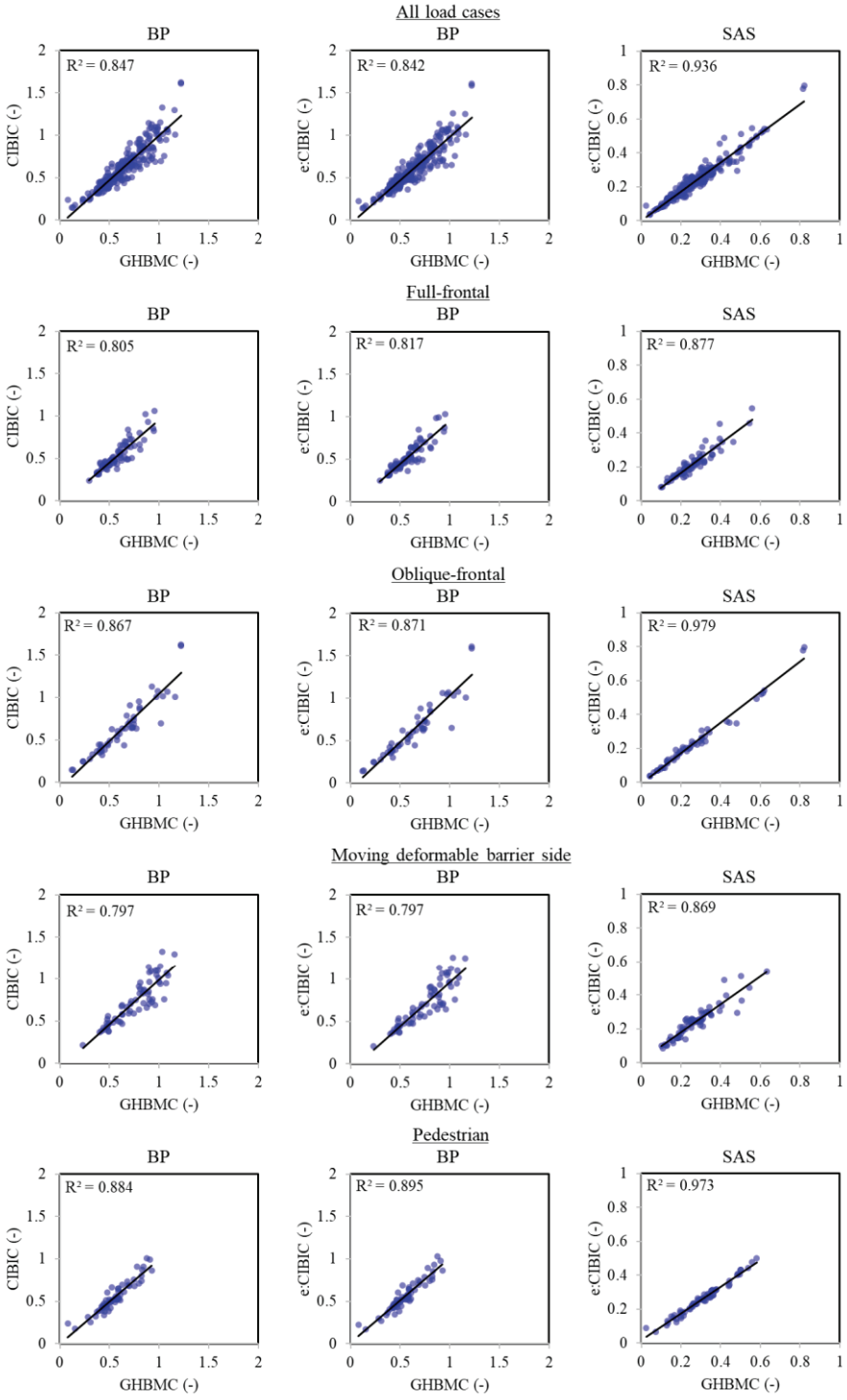

Figure 9. Correlation plots of the peak resultant value of the MPS between the GHBMC model and CIBIC/e:CIBIC

Table 2.
Summary of coefficient of determination (R^2)

Load case	MPS in BP GHBMC v.s. CIBIC	MPS in BP GHBMC v.s. e:CIBIC	MPS in SAS GHBMC v.s. e:CIBIC
All load case	0.847	0.842	0.936
Full-Frontal	0.805	0.817	0.877
Oblique-frontal	0.867	0.871	0.979
MDB side	0.797	0.797	0.869
Pedestrian	0.884	0.895	0.973

Figures 10 through 12 respectively compare the time histories of the MPS in the BP predicted by the CIBIC criterion, the MPS in the BP predicted by the e:CIBIC criterion and the MPS in the SAS predicted by the e:CIBIC criterion, all against those predicted for the corresponding measure by the GHBMC head/brain model. The solid and the dotted curve represent the results from the injury criteria and those from the GHBMC head/brain model, respectively. Comparisons were made for one exemplar load case chosen from each of the full-frontal, oblique-frontal, moving deformable barrier side and pedestrian impact load cases used for validation. For each of these three comparisons, Table 3 summarizes the average of the CORA metric over all the load cases included in each of the four crash configurations along with the overall average of the 246 load cases.

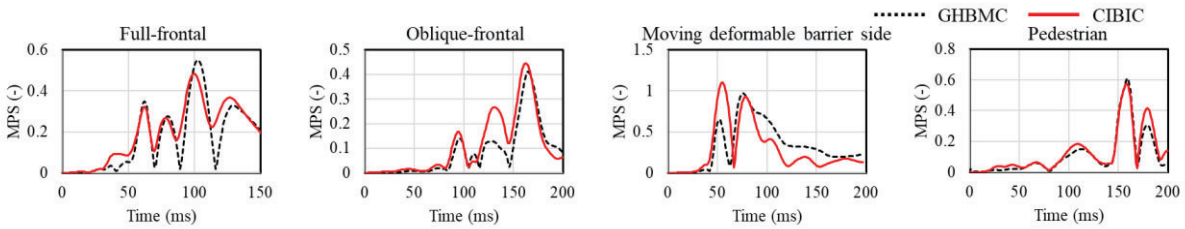

Figure 10. Comparison of the time history of the MPS in the BP between CIBIC and the GHBMC model

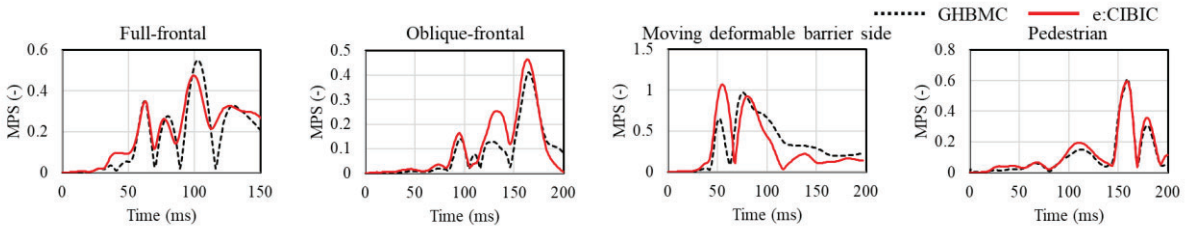

Figure 11. Comparison of the time history of the MPS in the BP between e:CIBIC and the GHBMC model

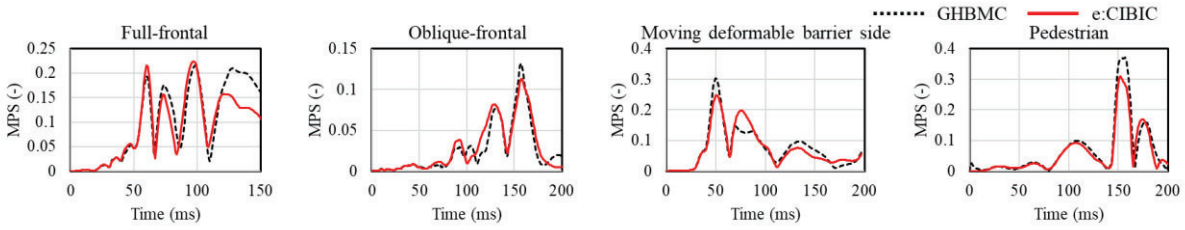

Figure 12. Comparison of the time history of the MPS in the SAS between e:CIBIC and the GHBMC model

Table 3.
Summary of the average value of the CORA metric

Load case	MPS in BP GHBMC v.s. CIBIC	MPS in BP GHBMC v.s. e:CIBIC	MPS in SAS GHBMC v.s. e:CIBIC
All load case	0.736	0.733	0.852
Full-Frontal	0.741	0.735	0.861
Oblique-frontal	0.728	0.728	0.833
MDB side	0.657	0.658	0.840
Pedestrian	0.819	0.815	0.872

DISCUSSION

In an effort to predict rupture of the BV and subsequent ASDH, a methodology of prediction using a practical, kinematics-based injury criterion was investigated. To the best of the authors' knowledge, this is the first attempt to establish such a simplified injury criterion to predict strains in the BP and the SAS simultaneously. As the first step, the existing CIBIC criterion was extended to incorporate one more SLS in series to predict the MPS in the SAS, in addition to the MPS in the BP, given the assumption that the strain in the SAS is significantly related to the strain in the BVs due to strong connection between the SAT and the blood vessels running through the SAS. The results of the current study showed that this extended version of the CIBIC criterion, e:CIBIC, succeeded in simultaneously predicting both the MPS in the BP and the MPS in the SAS predicted by the GHBMC with a simplified model, while maintaining the prediction capability of the CIBIC criterion for the MPS in the BP, as summarized in Tables 2 and 3 for the coefficient of determination of the peak MPS correlation and the average CORA metric of the MPS time histories, respectively. Although promising results have been obtained in comparison with a specific full-FE head/brain model, it should be noted that the validity of the results largely depends on the validity of such head/brain model against which the model parameters are optimized. Further improvement of the kinematics-based simplified injury criterion needs to be considered as the full-FE head/brain models are improved.

The current study validated the e:CIBIC criterion with the model parameters optimized in three simplified load cases against a total of 246 head impacts from pedestrian, oblique-frontal, full-frontal and moving deformable barrier side crash tests or simulations. The results of the validation generally showed a trend of degradation of the prediction capability in this order of the impact configurations. This can be endorsed by the exemplar acceleration time histories presented in Figure 13. For each of the rotational acceleration time history plot, the rotational axis most relevant to the corresponding impact configuration was chosen (X-axis for pedestrian and MDB side, Y-axis for oblique-frontal and full-frontal). The duration superimposed on each of the plot represents the wavelength of the single or combined peak of the rotational acceleration deemed responsible for the largest peak response. The wavelengths were found to be approximately 15, 22, 65 and 70 ms for pedestrian, oblique-frontal, full-frontal and MDB side impact configurations, indicating that the prediction capability is degraded as the wavelength of the relevant peak goes up. Despite that the e:CIBIC criterion is based on the SLS that represents a viscoelastic material response, one set of the SLS only includes one single damping coefficient, which means that only one time constant is represented by each of the SLS. This would reduce the prediction capability as the impact duration becomes longer and a wider range of the frequency components is involved. A future study may need to consider the increase in the number of time constants represented in the simplified viscoelastic model.

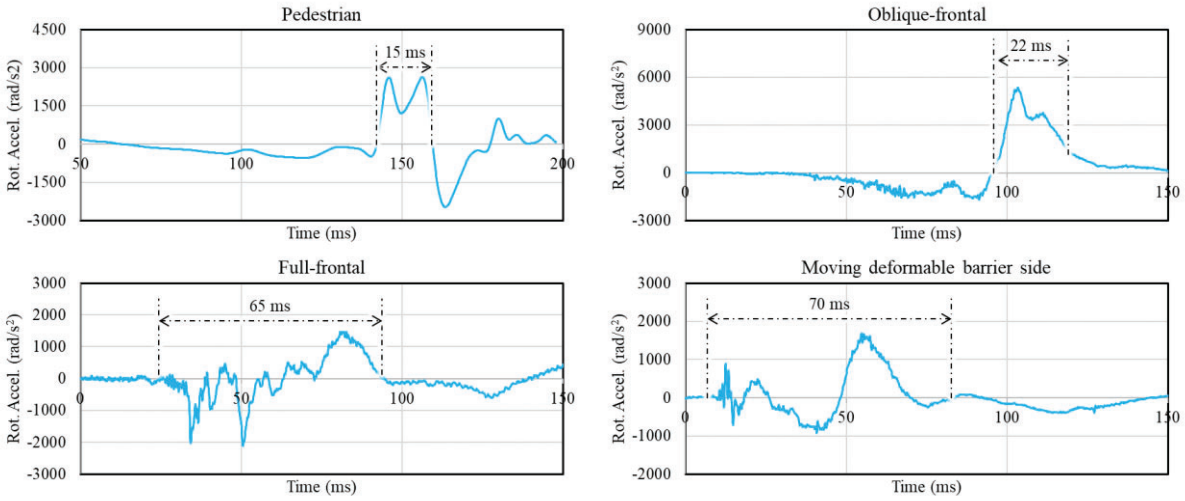

Figure 13. Rotational acceleration time histories of the head about the most relevant axis

The next step towards the ultimate goal of predicting the damage to the BP and the acute subdural hematoma with a practical simplified injury criterion, a detailed FE model of the head/brain that incorporate accurate geometry, material property and boundary conditions needs to be used to clarify and quantify the influence of the strain in the SAS on the strain in the BV. Once such clarifications are given and the relationship between the strain in the SAS and the strain in the BV is established, the combination of the assessment criteria of both the head linear acceleration (such as HIC) and the rotational acceleration (such as e:CIBIC) would allow prediction of a variety of different brain injury types, including contusion, epidural hemorrhage, concussion/diffuse axonal injury, brain swelling and acute subdural hematoma.

CONCLUSIONS

In this study, the rotational brain injury criteria to predict the MPS in the BP, the CIBIC criterion, was enhanced by implementing another set of the SLS model in series to predict the MPS in the SAS in addition to the MPS in the BP. As a result, the following conclusions were reached:

- The six model parameters of the e:CIBIC criterion optimized for the three simplified head rotational acceleration time histories resulted in the coefficient of determination of 0.846 and 0.936 against the GHBMC head/brain model for the peak values of the MPS in the BP and the MPS in the SAS, respectively, in the validation using a total of 246 crash tests and simulations that included four different impact configurations.
- The results compared against the CIBIC criterion with the coefficient of determination of 0.849 for the MPS in the BP, showing that the e:CIBIC criterion is capable of predicting the MPS in the SAS, while maintaining the predictive capability of the CIBIC criterion for the MPS in the BP.
- The overall average CORA metric obtained from the model validation were 0.732 and 0.852 against the GHBMC head/brain model for the time histories of the MPS in the BP and the MPS in the SAS, respectively, confirming the same trend as that of the peak MPS correlation against the CIBIC criterion that yielded the overall average CORA metric of 0.734 for the MPS in the BP.
- The validation results for each of the impact configurations showed a generic trend of degradation in the predictive capability as the wavelength of the rotational acceleration time history responsible for the overall peak response becomes longer, requiring further investigations on the influence of the number of time constants represented by the model.

REFERENCES

[1] International Transport Forum. 2021. “Road Safety Annual Report 2021: The Impact of Covid-19.” OECD Publishing, Paris.

[2] National Police Agency. (2022, March 3). Table Number 1-3, Trends in traffic accidents by year (1948-2021). Traffic Accident Statistics, Annual Report 2021 (Traffic accidents). https://www.npa.go.jp/publications/statistics/koutsuu/toukeihyo_e.html

[3] National Police Agency. (2022, March 3). Table Number 2-4-2, Casualties by major part of physical damage and road user type. Traffic Accident Statistics, Annual Report 2021 (Serious accidents). https://www.npa.go.jp/publications/statistics/koutsuu/toukeihyo_e.html

[4] Li, M., Zhao, Z., Yu, G. and Zhang, J. 2016. “Epidemiology of traumatic brain injury over the world: a systematic review.” General medicine: open access 2016; 4(5): e275

[5] Takahashi, Y. and Yanaoka, T. 2017. “A study of injury criteria for brain injuries in traffic accidents.” In proceedings of the 25th ESV conference (Detroit, MI, USA, June 5-8), paper number 17-0040

[6] Holbourn, A.H.S. 1943. “Mechanics of head injuries.” Lancet 2. October 9: 438–41

[7] Laic, R., Kapeliotis, M., Famaey, N., Depreitere, B., Kleiven, S. and Sloten, J. 2021. “Quantifying biovariability in position and diameter of bridging veins to improve acute subdural hematoma prediction in FE head models.” In proceedings of the IRCOBI conference 2021 (online), paper number IRC-21-41

[8] Fernandes, S., Sousa, R. and Ptak, M. 2021. “Numerical Aspects of Subdural Haematoma Modeling and Prediction.” In proceedings of the IRCOBI conference 2021 (online), paper number IRC-21-43

[9] Mao, H., Zhang, L., Jiang, B., Genthikatti, V.V., Jin, X., Zhu, F., Makwana, R., Gill, A., Jandir, G., Singh, A., Yang, K.H. 2013. “Development of a finite element human head model partially validated with thirty five experimental cases.” J Biomech Eng., 135(11): 111002

[10] Gabler, L., Crandall, J. and Panzer, M.. 2019. “Development of a Second-Order System for Rapid Estimation of Maximum Brain Strain.” Ann Biomed Eng. 2019 Sep; 47(9):1971-1981

[11] Shafique, S., Rayi, A. 2022. “Anatomy, Head and Neck, Subarachnoid Space. [Updated 2022 Aug 8].” In: StatPearls [Internet] (StatPearls Publishing, Treasure Island, FL, 2022 Jan-). https://www.ncbi.nlm.nih.gov/books/NBK557521/

[12] Mortazavi, M., Quadri, S., Khan, M., Gustin, A., Suriya, S., Hassanzadeh, T., Fahimdanesh, K., Adl, F., Fard, S., Taqi, M., Armstrong, I., Martin, B. and Tubbs, R. 2018. “Subarachnoid Trabecurae: A Comprehensive Review of Their Embryology, Histology, Morphology, and Surgical Significance.” World Neurosurg. (2018) 111:279-290

[13] National Highway Traffic Safety Administration. “Vehicle Crash Test Database.” https://www.nhtsa.gov/research-data/research-testing-databases#/vehicle

[14] MathWorks. 2019. “MATLAB/Simulink.” https://jp.mathworks.com/products/simulink.html

[15] ESTECO SpA. 2022. “modeFRONTIER.” https://engineering.esteco.com/modefrontier/

[16] ISO. 2014. “ISO/TS 18571:2014 Road vehicles - Objective rating metric for non-ambiguous signals”

[17] ISO. 2021. “ISO/TR 19222:2021 Road vehicles - Injury risk curves for the THOR dummy”

EFFECT OF SEAT BELT USE AND AIRBAGS DEPLOYMENT ON CLINICAL OUTCOMES IN ROAD TRAFFIC INJURY PATIENTS

SHORT TITLE: EFFECT OF SAFETY DEVICES

Jong Hee Kim, MD [a]

Gwan Jin Park, MD [a]

In Chan Shin [a]

Seung Min Yong [a]

Young Min Kim, MD [a]

Hyun Seok Chai, MD [a]

Sang Chul Kim, MD, PhD [a]

Hoon Kim, MD, PhD [a]

Suk Woo Lee, MD, PhD [a]

[a]Department of Emergency Medicine, Chungbuk National University Hospital, Cheongju, Korea
776, 1st Sunwhan-ro, Seowon-gu, Cheongju-si, Chungcheongbuk-do 28646, Korea

Address for Correspondence

Gwan Jin Park, MD

Department of Emergency Medicine, Chungbuk National University Hospital,
776, 1st Sunwhan-ro, Seowon-gu, Cheongju-si, Chungcheongbuk-do 28646, Korea
Phone: +82-10-7477-3293
FAX: +82-043-269-7810
E-mail: pkj83531@naver.com

Page Number 23-0262

ABSTRACT

Objective: Seat belts and airbags are safety devices designed to prevent road traffic injuries (RTI). They reduce fatal outcomes in patients with RTI. This study aimed to compare their effectiveness on the clinical outcomes of injured patients with RTI.

Methods and Data sources: A multicenter cross-sectional study was conducted using the Emergency Department-based Injury In-depth Surveillance (EDIIS) registry between Jan 2011 and Dec 2020. All patients who sustained RTI in a vehicle with fewer than 10 seats were eligible. The target population was categorized into four groups: seat belt use and airbag deployment, seat belt use only, airbag deployment only, and non-use. The primary outcome was intracranial injury. The secondary and tertiary outcomes were intensive care unit (ICU) admission and in-hospital mortality. The adjusted odds ratios (AORs) (95% confidence intervals [Cis]) of the safety device for related outcomes were calculated.

Results: Among 82,262 patients, 13,929 (16.9%) were classified as seatbelt and airbag deployment; 47,123 (57.4%) as seatbelt use only; 1,820 (2.2%) as airbag deployment only; and 19,300 (23.5%) as the non-use group. Compared to the non-use group, AORs (95% CIs) for intracranial injury were 0.49 (0.42-0.56) in the seat belt use and airbag deployment groups, 0.39 (0.35-0.44) in the seat belt use only group, and 1.34 (1.08-1.67) in the airbag deployment only group. For in-hospital mortality, AORs were 0.29 (0.22-0.36) in the seat belt use and airbag deployment groups, 0.17 (0.14-0.21) in the seat belt use only group, and 1.74 (1.30-2.32) in the airbag deployment only group.

Conclusion: Seat belt use had a significant preventive effect on intracranial injury and in-hospital mortality. The airbag deployment only group had worse outcomes. Public efforts to increase the proper use of safety devices are needed to reduce the RTI burden.

Keywords: Accidents, Traffic, Seat Belts, Air Bags, Brain Injuries

INTRODUCTION

Death from road traffic injury (RTI) increased to 1.35 million annually in 2016 and is now the eighth leading cause among all age groups.[1] In Korea, the number of deaths from RTI in 2020 was 3,081, and the overall trend over the decade has been decreasing since 2012.[2] However, it is considered the leading cause of death for children and young adults aged 5-29 years, and low- and middle-income countries bear the greatest burden of road traffic fatalities and injuries.[1,3] Most patients who survive RTI suffer from severe disabilities and economic costs, resulting in a public health burden.[4] Several strategies have been implemented to reduce RTI: road safety campaigns such as seatbelt use, reducing alcohol-impaired driving, various safety technologies such as seatbelts, airbags, child safety seats, electronic stability control, and strong law enforcement.[5-7]

Seat belt use is considered the most effective modality to save lives. When properly used, it can reduce the risk of fatal injury by 45% and moderate-to-critical injury by 50%.[6.8] However, seat belt use rates varied widely across countries. Seat belt use increased to 89.6% in 2018 in the United States, but in developing countries, it remained low at less than 60%.[8-10] According to the 2021 Report on the Transport Culture Index of Korea, seatbelt use rates increased from 73% in 2011 to 87% in 2017, but remained at a standstill of 84% in 2021.[11]

Airbags have been introduced to provide further protection from RTI in severe collisions.[12,13] Frontal airbags saved 50,457 lives from 1987 to 2017 in the United States and reduced fatalities by 14% when seat belts were not used.[8] However, severe studies reported that, regarding air-bag-related injuries, unstrained drivers in frontal collisions were more likely to sustain more severe injuries.[13-15]

Each device is well known to reduce fatal outcomes in patients with RTI and has been implemented with a safety device designed to prevent injuries. However, studies comparing the preventive effects of seat belts and airbags on clinical outcomes are limited. This study aimed to compare the effectiveness of these safety devices on the clinical outcomes of injured patients with RTI.

METHODS

Study design and setting, data source

This was a multicenter cross-sectional observational study using the Emergency Department-based Injury In-depth Surveillance (EDIIS) database in Korea. The EDIIS is a nationwide prospective database of injured

patients visiting the ED, supported by the Korea Centers for Disease Control and Prevention (CDC). It was established in five hospitals in 2006, and currently, 23 EDs gather injury-related information for injury prevention. EDIIS was constructed based on the core dataset of the International Classification of External Causes of Injuries by the World Health Organization. The database comprises 58 items, including the patient's demographics, injury-related information, emergency medical service (EMS) records, clinical findings, diagnosis and medical treatment in the ED, and clinical outcomes. Primary surveillance data were collected by general physicians in each ED, and the recorded data were regularly supervised and revised by emergency physicians and trained research coordinators. All research coordinators were required to complete training before participation and upload the surveillance data into a web-based database system of the KOREA CDC. For quality assurance, the data were reviewed monthly by a quality management committee.[16]

Study population

The study population included all injured patients who sustained RTI in the vehicle and visited the ED between January 2011 and December 2020. We excluded cases resulting from out-of-vehicle RTI, 10 or more passenger vehicles, children aged six years (they are obliged to use safety car seats in Korean law), or had unknown information on seat belt use, airbag deployment, and clinical outcomes.

Main outcomes

The primary outcome was intracranial injury, which was defined as the diagnosis code of the ICD-10 from S06.1 to S06.9. The diagnosis code is recorded on a discharge summary after an ED or hospital admission. The secondary and tertiary outcomes were intensive care unit (ICU) admission and in-hospital mortality. The latter was defined as death in the ED or during admission for injury care determined at discharge from the ED or hospital.

Variables and measurements

The main exposure variables were seat belt use and airbag deployment, as indicated in the EDIIS registry. The study population was categorized into four groups: seat belt use and airbag deployment, seat belt use only, airbag deployment only, and non-use. We collected information on demographic variables (age, sex, and past medical history), day of injury (weekend and weekday), time of injury (day [06:00–18:00]), alcohol use, EMS use, injury-related variables (driving status, type of road [expressway, national way, alleyway, and others], collision direction (frontal, lateral, rear, rollover, complex, and others), anatomical location of injury), excess mortality ratio-based injury severity score (EMR-ISS), and hospital-related variables (time interval from injury to ED arrival, initial mental status and vital signs at the ED, length of ED stay, ED outcome, and in-hospital mortality).

Statistical analysis

Counts and proportions were used for categorical variables, and medians and interquartile ranges (IQR) for continuous variables. We used the Kruskal-Wallis test for continuous variables and Pearson's χ^2 test for categorical variables. Adjusted odds ratios (AORs) (95% confidence intervals [Cis]) of seat belt use and airbag deployment for related outcomes were calculated using multivariable logistic regression analysis. A two-sided *P* value of < 0.05 was defined as significant. All statistical analyses were performed using the SAS software (version 9.4; SAS Institute Inc., Cary, NC, USA).

Ethics statement

This study was approved by the Institutional Review Board (IRB) of the Chungbuk National University Hospital (IRB No. 2022-10-013). The requirement for informed consent was waived, and patient information was anonymized before analysis**.**

RESULTS

Of the 2,627,450 injured patients, 429,501 visited the ED because of road traffic injuries. A total of 82,262 patients were included in the analysis, excluding out-of-vehicle injuries (n=88,576), in-vehicle injuries with more than 10 seats (n=161,041), children aged below six years (n=8,209), unknown outcomes (n=41), seat belt use (n=22,742), and airbag deployment (Figure 1).

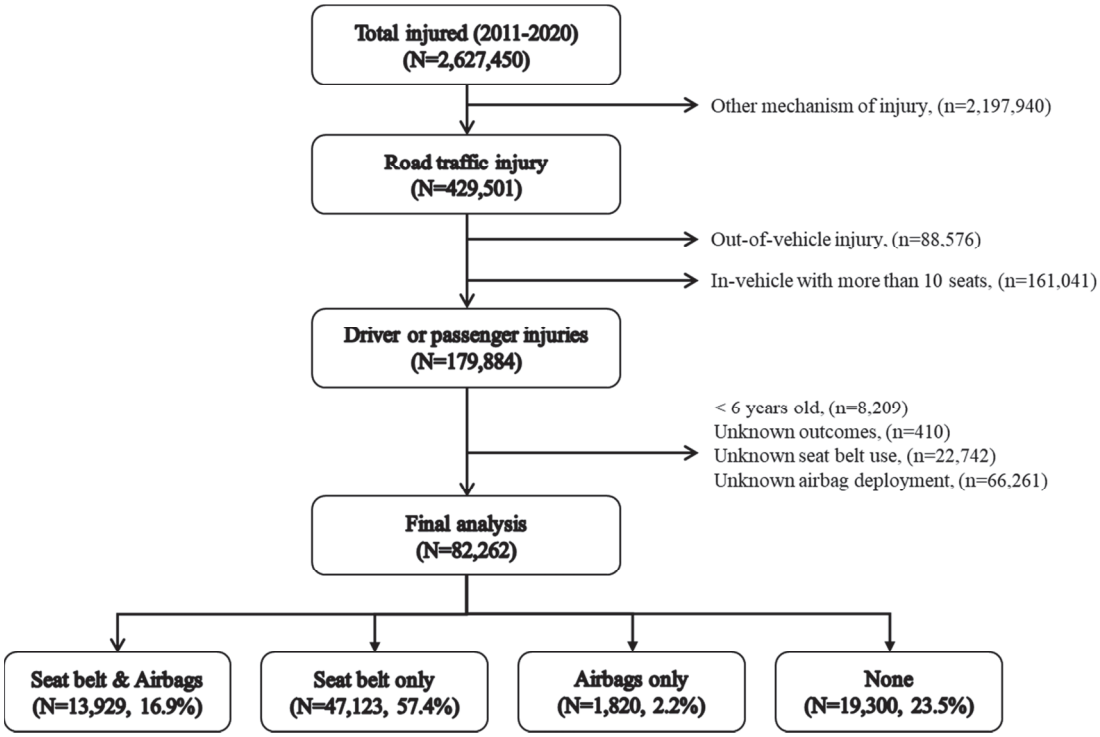

Figure 1. Study population.

Table 1 shows the demographic characteristics of the study population using safety devices. Among 82,262 eligible patients, there were 13,929 (16.9%) in the seat belt use and airbag deployment group, 47,213 (57.4%) in the seat belt use only group, 1,820 (2.2%) in the airbag deployment only group, and 19, 300 (23.5 %) in the non-use group. The airbag deployment only group was more likely to be younger (median age, 34 years), injured at night (18:00-06:00), drink more alcohol (20.8%), use more EMS (64.0%), and show a decreased mental status at the ED visit (all P<0.001).

Table 1.
Demographic findings of study population by safety devices

	Total		**Seat belt and airbag**		**Seat belt only**		**Airbag only**		**None**		
	N	%	N	%	N	%	N	%	N	%	p-value
All	82262		13929	16.9	47213	57.4	1820	2.2	19300	23.5	
Age											<0.001
<18	3616	4.4	230	1.7	1369	2.9	102	5.6	1915	9.9	
18-30	17610	21.4	2892	20.8	9099	19.3	589	32.4	5030	26.1	
30-45	26619	32.4	4398	31.6	16405	34.7	540	29.7	5276	27.3	
45-65	26582	32.3	5006	35.9	16089	34.1	458	25.2	5029	26.1	
>65	7835	9.5	1403	10.1	4251	9.0	131	7.2	2050	10.6	
Median (IQR), year	40 (29-54)		42 (31-55)		41 (31-53)		34 (25-49)		36 (25-53)		<0.001
Sex											<0.001
Male	42053	51.1	8129	58.4	23897	50.6	1107	60.8	8920	46.2	
Day of injury											<0.001
Weekend	29264	35.6	4911	35.3	16533	35.0	605	33.2	7215	37.4	
Time of injury											<0.001
06:00-18:00	50431	61.3	7955	57.1	30742	65.1	845	46.4	10889	56.4	

18:00-06:00	31831	38.7	5974	42.9	16471	34.9	975	53.6	8411	43.6	
Past medical history											
Hypertension	2400	2.9	435	3.1	1358	2.9	55	3.0	552	2.9	0.448
Diabetes mellitus	1225	1.5	232	1.7	719	1.5	28	1.5	246	1.3	0.024
Chronic liver disease	151	0.2	32	0.2	77	0.2	5	0.3	37	0.2	0.309
Cerebrovascular disease	192	0.2	32	0.2	115	0.2	4	0.2	41	0.2	0.897
Alcohol consumption											<0.001
Yes	4325	5.3	820	5.9	1229	2.6	378	20.8	1898	9.8	
EMS use											
Yes	32579	39.6	7408	53.2	15586	33.0	1164	64.0	8421	43.6	<0.001
Mental status at the ED											<0.001
Alert	79074	96.1	13355	95.9	45908	97.2	1600	87.9	18211	94.4	
Verbal	873	1.1	191	1.4	264	0.6	77	4.2	341	1.8	
Painful stimuli	453	0.6	103	0.7	103	0.2	44	2.4	203	1.1	
Unresponsive	454	0.6	82	0.6	97	0.2	63	3.5	212	1.1	
Unknown	1408	1.7	198	1.4	841	1.8	36	2.0	333	1.7	
Vital signs											
SBP, Median (IQR)	133 (120-150)		136 (120-151)		135 (120-150)		130 (114-147)		130 (118-146)		<0.001
HR, Median (IQR)	82 (74-91)		83 (75-93)		81 (74-90)		86 (76-97)		82 (75-93)		<0.001
RR, Median (IQR)	20 (18-20)		20 (18-20)		20 (18-20)		20 (18-20)		20 (18-20)		<0.001

IQR, interquartile range; EMS, emergency medical services; ED, emergency department; SBP, systolic blood pressure; HR, heart rate; RR, respiratory rate.

The proportion of passengers was highest in the non-use group (70.1%). Frontal collision was the most common in the seat belt use and airbag deployment and airbag deployment only groups (19.8% and 24.8%, respectively). Regarding the anatomical classification of injury, the proportion of head and face injuries was higher in the airbag deployment only group and the non-use group (57.0% and 50.6%, respectively). However, a neck injury was most common in the seat belt use alone group (42.6%). The airbag deployment only group had a higher proportion of injury severity score, intracranial injury, ICU admission, and in-hospital mortality (all P<0.001; Table 2).

Table 2.
Injury-related characteristics by safety devices

	Total		**Seat belt and airbag**		**Seat belt only**		**Airbag only**		**None**		
	N	%	N	%	N	%	N	%	N	%	p-value
All	82262		13929	16.9	47213	57.4	1820	2.2	19300	23.5	
Driving status											<0.001
Driver	49759	60.5	10804	77.6	32115	68.0	1073	59.0	5767	29.9	
Passenger	32503	39.5	3125	22.4	15098	32.0	747	41.0	13533	70.1	
Type of road											<0.001
Expressway	14143	17.2	2991	21.5	8228	17.4	264	14.5	2660	13.8	
National way	64073	77.9	10363	74.4	37131	78.6	1430	78.6	15149	78.5	
Alleyway	1381	1.7	205	1.5	681	1.4	42	2.3	453	2.3	
Others	2665	3.2	370	2.7	1173	2.5	84	4.6	1038	5.4	
Collision direction											<0.001
Frontal	10712	13.0	2760	19.8	4603	9.7	451	24.8	2898	15.0	
Lateral	7431	9.0	1021	7.3	4163	8.8	132	7.3	2115	11.0	
Rear	13121	16.0	433	3.1	9432	20.0	44	2.4	3212	16.6	

Roll over	1262	1.5	206	1.5	580	1.2	28	1.5	448	2.3	
Complex	2658	3.2	422	3.0	1630	3.5	47	2.6	559	2.9	
Others	47078	57.2	9087	65.2	26805	56.8	1118	61.4	10068	52.2	
Anatomical classification of injury											
Head and face	33676	40.9	5311	38.1	17556	37.2	1037	57.0	9772	50.6	<0.001
Neck	29767	36.2	3509	25.2	20122	42.6	351	19.3	5785	30.0	<0.001
Chest	14729	17.9	4134	29.7	7197	15.2	476	26.2	2922	15.1	<0.001
Abdomen	19887	24.2	3146	22.6	12523	26.5	364	20.0	3854	20.0	<0.001
Upper extremity	14720	17.9	3150	22.6	7741	16.4	421	23.1	3408	17.7	<0.001
Lower extremity	13110	15.9	2866	20.6	6226	13.2	499	27.4	3519	18.2	<0.001
Injury severity											
EMR-ISS ≥ 9	49035	59.6	9030	64.8	25772	54.6	1409	77.4	12824	66.4	<0.001
EMR-ISS ≥ 16	18403	22.4	4194	30.1	8007	17.0	856	47.0	5346	27.7	<0.001
Median (IQR)	9 (4-14)		9 (4-17)		9 (4-12)		13 (9-25)		9 (4-17)		<0.001
ED disposition											<0.001
Discharge	66827	81.2	10101	72.5	40780	86.4	1085	59.6	14861	77.0	
Transfer to other hospital	3504	4.3	780	5.6	1520	3.2	172	9.5	1032	5.3	
Admission	11592	14.1	2991	21.5	4845	10.3	518	28.5	3238	16.8	
Death	339	0.4	57	0.4	68	0.1	45	2.5	169	0.9	
Time interval from injury to ED arrival											
Median (IQR), hour	1.1 (0.6-3.7)		1.0 (0.6-2.8)		1.2 (0.7-4.3)		1.0 (0.5-2.1)		1.0 (0.6-3.0)		<0.001
ED length of stay											
Median (IQR), hour	1.9 (1.1-3.6)		2.5 (1.4-4.5)		1.7 (1.1-3.1)		3.1 (1.7-5.9)		2.1 (1.2-4.2)		<0.001
Clinical outcomes											
Intracranial injury	1902	2.3	334	2.4	731	1.5	107	5.9	730	3.8	<0.001
ICU admission	3287	4.0	960	6.9	1119	2.4	222	12.2	986	5.1	<0.001
In-hospital mortality	566	0.7	108	0.8	137	0.3	65	3.6	256	1.3	<0.001

EMR-ISS, excess mortality ratio-adjusted injury severity score; IQR, interquartile range; ED, emergency department; ICU, intensive care unit.

Figure 2 shows the trends in the applied safety devices by year. In the non-use group, it decreased from 29.3% in 2011 to 15.1% in 2020. The seat belt use rate reached approximately 82% by 2020. Compared to the non-use group, AORs (95% CIs) for intracranial injury were 0.49 (0.42-0.56) in the seat belt use and airbag deployment group, 0.39 (0.35-0.44) in the seat belt use only group, and 1.34 (1.08-1.67) in the airbag deployment only group. For ICU admission, AORs were 0.44 (0.40-0.48) in the seat belt use only group, and 2.02 (1.72-2.37) in the airbag deployment only group. For in-hospital mortality, AORs were 0.29 (0.22-0.36) in the seat belt use and airbag deployment group, 0.17 (0.14-0.21) in the seat belt use only group, and 1.74 (1.30-2.32) in the airbag deployment only group (Table 3).

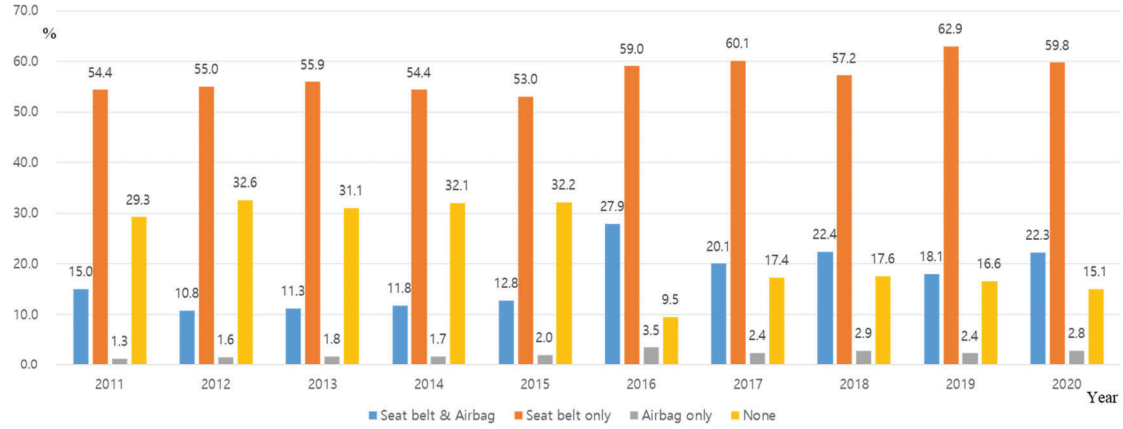

Figure 2. Trends in the applied safety devices by the year.

Table 3. Multivariable logistic regression analysis on study outcomes by safety devices

	Total	Positive outcomes		Unadjusted	Adjusted
	N	N	%	OR (95% CI)	OR (95% CI)
Primary outcome: Intracranial injury					
Total	82262	1902	2.3		
Seat belt and airbag	13929	334	2.4	0.63 (0.55-0.71)	0.49 (0.42-0.56)
Seat belt only	47213	731	1.5	0.40 (0.36-0.44)	0.39 (0.35-0.44)
Airbag only	1820	107	5.9	1.59 (1.29-1.96)	1.34 (1.08-1.67)
None	19300	730	3.8	1.00	1.00
Secondary outcome: ICU admission					
Total	82262	3287	4.0		
Seat belt and airbag	13929	960	6.9	1.38 (1.25-1.51)	1.08 (0.97-1.19)
Seat belt only	47213	1119	2.4	0.45 (0.41-0.49)	0.44 (0.40-0.48)
Airbag only	1820	222	12.2	2.58 (2.21-3.01)	2.02 (1.72-2.37)
None	19300	986	5.1	1.00	1.00
Tertiary outcome: In-hospital mortality					
Total	82262	566	0.7		
Seat belt and airbag	13929	108	0.8	0.58 (0.46-0.73)	0.29 (0.22-0.36)
Seat belt only	47213	137	0.3	0.22 (0.18-0.27)	0.17 (0.14-0.21)
Airbag only	1820	65	3.6	2.76 (2.09-3.63)	1.74 (1.30-2.32)
None	19300	256	1.3	1.00	1.00

Adjusted for age, sex, time of injury, diabetes mellitus, driving status, type of road, collision direction, alcohol consumption, and EMS use.

OR: odds ratio; CI: confidence interval; ICU: intensive care unit.

DISCUSSION

Through this injury surveillance data, we found that seat belt use and airbag deployment and seat belt use only had significant preventive effects on intracranial injury and in-hospital mortality because of RTI.

Seat belt use is well known to be the most effective modality for reducing fatalities from RTI. Among the numerous efforts to increase the seat belt use rate, mandatory seat belt legislation is highly effective in promoting wearing seat belts and a cost-effective measure to reduce the severity and sequelae of traumatic brain injuries related to RTI.[17,18] Among them, 71% of all countries have adopted the best practice of mandating the use of seat belts by front and rear seat occupants.[1] However, seat belt use rates did not increase further from the late 80% in developed countries and were found to be less than 60% in developing countries.[8,9] Various efforts have been made to increase the seat belt use rate beyond legislation, such as public campaigns and the development of new technologies such as belt reminders or interlocks.[1,19,20]

Airbags are regarded as supplemental safety measures that reduce the risk of injury from RTI in combination with seat belts. Despite using seat belts, car occupants are injured when they hit the vehicle's interior parts, such as the steering wheel or dashboard, and airbags reduce the level of contact.[8] Fatalities in frontal collisions, specifically airbags, have been reduced by 22% among belted drivers.[21] The United States has implemented the mandatory installation of airbags, but in Korea, there is no such obligation. However, vehicle manufacturers voluntarily installed airbags, and the installation rate of airbags in manufactured vehicles in Korea was 88.3% in 2003.[22]

Despite the reduced risk of injury from airbags, our results found that the deployment only group had worse outcomes: a higher proportion of decreased mentality at the ED and injury severity score were observed. Moreover, the proportion of intracranial injuries, ICU admissions, and in-hospital mortality were higher. Airbags are generally designed to inflate moderate-to-severe car crashes according to the direction and severity of the impact.[8] Unrestrained occupants are more likely to be positioned in the deployment path of the airbag during a collision, leading to higher lethality from the airbags.[13,15]

Numerous studies have shown an overall reduction in the number of fatalities in frontal collisions, mainly due to the reduced risk of serious head and neck injuries.[15,23] However, most studies included only car occupants who wore their seat belts in airbag-equipped vehicles. In this study, the head and face injury rate was 57% in the airbag deployment only group, but those in the seat belt use and airbag deployment group and seatbelt use only group were significantly lower (38.1% and 37.2%, respectively). These results reinforce that airbags are a complementary safety device rather than an alternative to seat belts. Considering that they are designed to be deployed during serious RTI, we ensured that all occupants were properly seated and wearing seat belts to reduce the risk of injury.

Another point was to identify the characteristics of the airbag deployment only group. In our results, they are more likely to be younger, injured at night, drink more alcohol, and use more EMS. Previous studies have noted that a higher risk of injury is associated with the physique of occupants or specific positions of occupant seating, specifically those who were unrestrained or improperly restrained.[13,24] Unrestrained drivers were more likely to use a cell phone while driving, drive at excessive speed limits, attempt to pass other vehicles, have alcohol-impaired driving, and not follow traffic rules.[25] The driver has the greatest influence on passenger seat belt use, and driver restraint use is a significant predictor of restraint use, specifically among young passengers in RTI.[26] Therefore, public efforts are needed to prevent fatal RTIs by spreading traffic safety awareness and implementing a desirable driving culture for car occupants.

This study had several limitations. First, this was a retrospective observational study, and there might have been potential confounders that influenced the exposure and outcomes. Injury-related data, which can influence outcomes such as the speed at the time of collision, counterparts of the RTI, and passengers' seating positions, were not available from the EDIIS registry. Second, seat belt use and airbag deployment, which were the main exposure variables, were ascertained only through face-to-face interviews with the patient and guardians. This might be subject to over- and underestimation, which can also result in bias. Furthermore, we only had information on whether the airbags were deployed. Airbag-related data, such as the type, number, and location of airbags embedded in the vehicle, were limited, and could not be used for analysis.

CONCLUSION

Seat belt use showed preventive effects on intracranial injury and in-hospital mortality from RTI. Airbag deployment without seatbelt use had no preventive effect on the clinical outcomes. These results suggest that airbags are not a substitute for seatbelts but are an additional device to reduce RTI. Public health efforts are needed to increase the proper use of safety devices and implement a good driving culture for car occupants, which can help reduce the health burden of RTI.

Disclosure

The authors have no potential conflicts of interest to disclose.

Author Contributions

Conceptualization: Kim JH and Park GJ. Methodology: Park GJ. Formal analysis: Kim JH and Park GJ. Investigation: Kim JH, Shin IC, and Yong SM. Data curation: Kim JH and Park GJ. Writing – original draft preparation: Kim JH and Park GJ. Writing – reviewing and editing: Park GJ, Kim YM, Chai HS, Kim SC, Kim H, and Lee SW.

REFERENCES

[1] World Health Organization. 2018. Global status report on road safety 2018: summary.
[2] Traffic Accident Analysis System. Traffic accident statistics. 2021. Korea ROAD traffic authority. Wonju-Si. [cited 2022 Sep 18]. Available from: http://taas.koroad.or.kr/web/bdm/srs/selectStaticalReportsList.do?menuId=WEB_KMP_IDA_SRS_TAA.
[3] Nantulya, V.M. and Reich, M.R. 2002. The neglected epidemic: Road traffic injuries in developing countries. BMJ, 324(7346), 1139-41.
[4] Global, regional, and national incidence, prevalence, and years lived with disability for 328 diseases and injuries for 195 countries, 1990-2016: a systematic analysis for the Global Burden of Disease Study 2016.2017. Lancet, 390(10100), 1211-59.
[5] Fisa, R., Musukuma, M., Sampa M, et al. 2022. Effects of interventions for preventing road traffic crashes: an overview of systematic reviews. BMC Public Health, 22(1):513.
[6] Kahane, C.J. 2015. Lives saved by vehicle safety technologies and associated Federal Motor Vehicle Safety Standards, 1960 to 2012–Passenger cars and LTVs–With reviews of 26 FMVSS and the effectiveness of their associated safety technologies in reducing fatalities, injuries, and crashes. Report No DOT HS, 812:069.
[7] Bhalla, K., and Gleason, K. 2020. Effects of vehicle safety design on road traffic deaths, injuries, and public health burden in the Latin American region: A modelling study. Lancet Glob Health, 8(6):e819-e28.
[8] National Center for Statistics and Analysis. Occupant protection in passenger vehicles:2018 data (Traffic Safety Facts) Report No. DOT HS 812 967). National Highway Traffic Safety Administration, 2020 [cited 2022 Sep 23]. Available from: https://crashstats.nhtsa.dot.gov/Api/Public/ViewPublication/812967.pdf.
[9] Vecino-Ortiz, A.I., Bishai, D., Chandran, A., et al. 2014. Seatbelt wearing rates in middle-income countries: A cross-country analysis. Accid Anal Prev. 71:115-9.
[10] Ojo, T.K. 2018. Seat belt and child restraint use in a developing country metropolitan city. Accid Anal Prev. 113:325-9.
[11] The Korea Transportation Safety Authority. Report on Transport Culture Index of Korea, 2021. Gimcheon-si. 2022. [cited 2022 Sep 17]. Available from: https://www.kotsa.or.kr/portal/bbs/transafe_view.do?bbscCode=transafe&cateCode=&bbscSeqn=5402&pageNumb=1&sechCdtn=0&sechKywd=%EA%B5%90%ED%86%B5%EB%AC%B8%ED%99%94%EC%A7%80%EC%88%98+%EC%8B%A4%ED%83%9C%EC%A1%B0%EC%82%AC&menuCode=05070000.
[12] Stewart, T.C., Girotti, M.J., Nikore, V., Williamson, J. 2003. Effect of airbag deployment on head injuries in severe passenger motor vehicle crashes in Ontario, Canada. J Trauma, 54(2), 266-72.
[13] the Royal Society for the Prevention of Accidents. Road Safety Factsheet. Airbags Factsheet. 2021. [cited 2022 Sep 25]. Available from: https://www.rospa.com/rospaweb/docs/advice-services/road-safety/vehicles/airbags-factsheet.pdf.
[14] Corazza, M., Trincone, S., Virgili, A. 2004. Effects of airbag deployment: lesions, epidemiology, and management. Am J Clin Dermatol, 5(5),295-300.
[15] Wallis, L.A., and Greaves, I. 2002. Injuries associated with airbag deployment. Emergency Medicine Journal, 19(6),490-3.
[16] Park, G.J., Shin, J., Kim, S.C., et al. 2019. Protective effect of helmet use on cervical injury in motorcycle crashes: A case-control study. Injury. 50(3), 657-62.
[17] Lee, L.K., Monuteaux, M.C., Burghardt, L.C., et al. 2015. Motor Vehicle Crash Fatalities in States With Primary Versus Secondary Seat Belt Laws: A Time-Series Analysis. Ann Intern Med, 163(3),184-90.
[18] Costich, J.F., and Slavova, S.S. 2015. Using Enforcement and Adjudication Data to Assess the Impact of a Primary Safety Belt Law. Traffic Inj Prev, 16(7),664-8.
[19] Kidd, D.G., McCartt, A.T., et al. 2014. Attitudes toward seat belt use and in-vehicle technologies for encouraging belt use. Traffic Inj Prev, 15(1),10-7.
[20] Kidd, D.G., Singer, J. 2019. The effects of persistent audible seat belt reminders and a speed-limiting interlock on the seat belt use of drivers who do not always use a seat belt. J Safety Res. 71,13-24.
[21] Høye, A. 2010. Are airbags a dangerous safety measure? A meta-analysis of the effects of frontal airbags on driver fatalities. Accid Anal Prev, 42(6), 2030-40.
[22] Korea Consumer Agency. Passenger vehicle airbags safety survey. 2003. [cited 2022 Oct 11. Available from: https://www.kca.go.kr/smartconsumer/sub.do?menukey=7301&mode=view&no=1000338532.
[23] Barnes, J., Morris, A., Fildes, B. 2001. Airbag effectiveness in real world crashes.
[24] O'Donovan, S., van den Heuvel, C., Baldock, M., Byard, R.W. 2020. Injuries, death and vehicle airbag deployment. Med Sci Law. 60(2),147-9.
[25] Yagoub, U., Saiyed, N.S., Rahim, B.E.A., 2021. Road Traffic Injuries and Related Safety Measures: A Multicentre Analysis at Military Hospitals in Tabuk, Saudi Arabia. Emerg Med Int, 6617381.
[26] Roehler, D.R., Elliott, M.R., Quinlan, K.P., et al. 2019. Factors Associated With Unrestrained Young

Passengers in Motor Vehicle Crashes. Pediatrics, 143(3).